Scuola Internazionale Superiore di Studi Avanzati - Trieste

$\mu \rightarrow e\gamma$ and $\tau \rightarrow \mu\gamma$ in supersymmetric models

Thesis submitted for the degree of Doctor Philosophiæ

CANDIDATE:

Carlos E. Yaguna

SUPERVISOR:

Prof. Serguey Petcov

SISSA – Via Beirut 2-4 – 34014 TRIESTE – ITALY

$\mu \to e\gamma$ and $\tau \to \mu\gamma$ in supersymmetric models

Thesis submitted for the degree of Doctor Philosophiæ

CANDIDATE:

Carlos E. Yaguna

SUPERVISOR:

Prof. Serguey Petcov

To Adriana

Acknowledgments

Without the support of Enrico Nardi I would not have come to SISSA. I thank him for this opportunity.

I thank to Antonio Masiero, Silvia Pascoli, Sudhir Vempati, and Yasutaka Takanishi with whom I collaborate. And to Stefano Bertolini for informal discussions.

I am grateful to my supervisor, Serguey Petcov, for his collaboration and his enduring encouragement.

Finally, I express my enormous gratitude to Stefano Profumo, with whom most of this research was done. I have learned a lot from him.

Contents

Introduction

Lepton flavor violating decays are a unique probe of new physics. They might be related to the mechanism of neutrino mass generation, to the spontaneous breaking of supersymmetry, or to new interactions at high energies, above and below the GUT scale. Their detection would give an unmistakable signal of physics beyond the Standard Model and its minimal extensions, and could be the first manifestation of supersymmetric effects. And it would certainly mark the beginning of a new era in particle physics.

Among them, $\mu \to e\gamma$ and $\tau \to \mu\gamma$ offer excellent experimental perspectives. The limits on these decays are already impressive and significant improvements are expected in the next few years. Thus, their role in constraining and perhaps discovering new physics will be reinforced by future experiments.

Recently, motivated by these experimental efforts, by the study of neutrino mass models, and by the data from ν oscillation experiments, $\mu \to e\gamma$ and $\tau \to \mu\gamma$ have received particular attention. Different aspects regarding these processes were investigated in papers [1, 2, 3, 4]. This thesis is based on those works.

In the first chapter, the motivation and the general framework are introduced. A critical review of some assumptions commonly employed in the computation of lepton flavor violating decays is presented in chapter two. We investigate, in the third chapter, the implications, within a particular $SO(10)$ model, of $\mu \to e\gamma$ and $\tau \to \mu\gamma$ for the determination of the viable parameter space, and we confront the perspectives for their detection against accelerator experiments in the search for supersymmetry. Finally, in chapter four we address the relevance of the gaugino spectrum on the computation of $BR(\mu \to e\gamma)$.

C.E.Y.

Chapter 1

General considerations

1.1 Experimental facts

The experimental results obtained so far in the search for lepton flavor violating processes are contrasting. In the charged lepton sector, where rare μ and τ decays offer the best possibilities to search for, such processes have never been observed. Strong bounds exist on those decays (table 1.1) and planned experiments are expected to improve them. On the contrary, the existence of flavor transitions among neutrinos have been demonstrated in oscillation experiments. Thus, they have established that the lepton flavor is not conserved.

Reactor, atmospheric and solar neutrino oscillation data are explained by the existence of neutrino mixing in the weak charged current. The neutrino

Decay	Experimental Limits	
	Present	Expected
$\mu \to e\gamma$	1.2×10^{-11}	10^{-13}-10^{-14}
$\tau \to \mu\gamma$	3.1×10^{-7}	1.0×10^{-8}
$\tau \to e\gamma$	3.7×10^{-7}	1.0×10^{-8}
$\mu \to 3e$	1.0×10^{-12}	
$\mu \to e\gamma\gamma$	7.2×10^{-11}	

Table 1.1: Experimental limits on lepton flavor violating decays

mixing matrix U relates flavor and mass eigenstate neutrinos according to

$$\nu_a = \sum_i U_{ai}\nu_i, \tag{1.1}$$

where ν_a $(a = e, \mu, \tau)$ denote flavor neutrinos and ν_i $(i = 1, 2, 3)$ denote mass eigenstates. Being unitary, U can be parameterized – ignoring phases – in terms of three mixing angles $\theta_{12}, \theta_{23}, \theta_{13}$ as

$$U = \begin{pmatrix} c_{13}c_{12} & c_{13}s_{12} & s_{13} \\ -c_{23}s_{12} - s_{23}s_{13}c_{12} & c_{23}c_{12} - s_{23}s_{13}s_{12} & s_{23}c_{13} \\ s_{23}s_{12} - c_{23}s_{13}c_{12} & -s_{23}c_{12} - c_{23}s_{13}s_{12} & c_{23}c_{13} \end{pmatrix}, \tag{1.2}$$

where we used the common notation $c_{ij} = \cos\theta_{ij}$, $s_{ij} = \sin\theta_{ij}$. Recent measurements indicate that $s_{23} \approx 1/\sqrt{2}$ and $s_{12} \approx 0.6$; on the third angle only an upper bound exists, $s_{13} < 0.2$. Hence, contrary to quarks, leptons feature large mixing angles.

Because they are sensitive to neutrino masses only through mass square differences, neutrino oscillation experiments cannot be used to determine the absolute values of neutrino masses. In fact, they are not known yet. Though the solar and the atmospheric neutrino mass square differences have been measured ($\Delta m^2_{solar} \approx 7 \times 10^{-5}\text{eV}^2$ and $\Delta m^2_{atm} \approx 3 \times 10^{-3}\text{eV}^2$, respectively), three types of neutrino spectra are compatible with them. They are

1. The hierarchical spectrum ($m_{\nu_1} \ll m_{\nu_2} \ll m_{\nu_3}$):

$$m_{\nu_1} \sim 0, \quad m_{\nu_2} = \sqrt{\Delta m^2_{solar}}, \quad m_{\nu_3} = \sqrt{\Delta m^2_{atm}}. \tag{1.3}$$

2. The quasi-degenerate spectrum ($m_{\nu_1} \sim m_{\nu_2} \sim m_{\nu_3}$):

$$m_{\nu_1} \equiv m_\nu, \quad m_{\nu_2} = m_\nu + \frac{1}{2m_\nu}\Delta m^2_{solar}, \quad m_{\nu_3} = m_\nu + \frac{1}{2m_\nu}\Delta m^2_{atm} \tag{1.4}$$

3. The inverse-hierarchical spectrum ($m_{\nu_1} \sim m_{\nu_2} \gg m_{\nu_3}$):

$$m_{\nu_1} = \sqrt{\Delta m^2_{atm}} - \frac{1}{2m_\nu}\Delta m^2_{solar}, \quad m_{\nu_2} = \sqrt{\Delta m^2_{atm}}, \quad m_{\nu_3} \simeq 0. \tag{1.5}$$

Additionally, an upper bound on the mass of the electron neutrino ($m_{\nu_e} \leq 2.2\text{eV}$) was obtained in tritium beta decay experiments and a cosmological limit on the sum of the masses of light neutrinos ($\sum m_{\nu_i} < 0.7\text{eV}$) was found by WMAP. Neutrinos, therefore, are much lighter than any other fermion in the Standard Model.

The good news is that, as a result of neutrino masses and mixing, the lepton flavor is not conserved. A departure from the Standard Model expectations has finally been found.

C.E.Y.

1.2 A standard approach

Can the Standard Model be extended to account satisfactorily for neutrino masses? Is such extension compatible with the experimental limits on LFV decays? The neutrino is the only known particle that, due to its neutrality, may have both a Majorana and a Dirac mass term. Yet, in the Standard Model, it has none. In fact, neutrinos can not have Dirac masses for right-handed neutrinos are not present, and a gauge invariant Majorana mass term is not renormalizable. But, if right-handed neutrinos are added to the Standard Model particle content, neutrinos will certainly acquire a mass.

To obtain Dirac type neutrinos, Majorana mass terms for right-handed neutrinos must be avoided, and imposing lepton number conservation is the simplest way of achieving it. Indeed, in contrast with the fermion number conserving Dirac masses, Majorana masses violate fermion number by two units. If neutrinos are Dirac particles, their mass matrix is

$$\mathbf{m}_D = v\mathbf{Y}_\nu, \tag{1.6}$$

being $\mathbf{Y}_\nu$ the matrix of neutrino Yukawa couplings and $v \sim 246$ GeV the electroweak symmetry breaking scale. The observed smallness of neutrino masses would then require unnaturally small values of the Yukawa couplings, $Y_\nu \lesssim 10^{-12}$.

The predictions for lepton flavor violating decays within this setup are not encouraging. For instance, the branching ratio of the decay $\mu \to e\gamma$

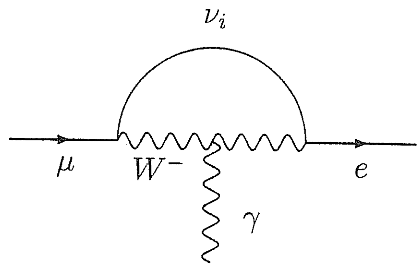

Figure 1.1: Feynman diagram for $\mu \to e\gamma$ in the Standard Model with massive neutrinos.

(fig 1.1) is extremely suppressed [5]

$$BR(\mu \to e\gamma) = \frac{3}{32}\frac{\alpha}{\pi}\left(\sum_i U^*_{\mu i}U_{ei}\frac{m^2_{\nu_i}}{m^2_W}\right)^2 \leq 10^{-50}. \tag{1.7}$$

The factor $(m^2_\nu/m^2_W)^2$ that renders it unobservable being the result of the leptonic GIM mechanism is a common feature for all LFV processes. The presence of neutrino masses therefore does not guarantee the observability of LFV decays.

If only the $SU(3) \times SU(2) \times U(1)$ gauge symmetry is required, then, because a Majorana mass term for right-handed neutrinos is allowed, neutrinos become Majorana particles. Moreover, their masses will naturally be smaller than those of any other particle in the Standard Model. Indeed, the light neutrino mass matrix turns out to be

$$\mathbf{m}_\nu = \mathbf{m}_D^T \mathbf{M}_\mathbf{R}^{-1} \mathbf{m}_D, \tag{1.8}$$

known as the see saw formula. Here, $\mathbf{m}_D$ is the Dirac mass matrix of neutrinos and $\mathbf{M}_\mathbf{R}$ is the Majorana mass matrix of right-handed neutrinos. Light neutrino masses are thus suppressed by the factor m_D/M_R with respect to their naive Dirac values.

Unfortunately, the rates of lepton flavor violating decays are as despairing as for Dirac neutrinos. $\mu \to e\gamma$, for example, proceeds through the same diagram (fig 1.1) but with six Majorana neutrinos running in the loop. Three of them are light and give the same GIM suppressed amplitude as before, and the other three, being predominantly right-handed, have suppressed couplings ($\sim m_D/M_R$) to the W boson, giving a negligible contribution.

The detection of lepton flavor violating decays, therefore, would be an unmistakable signal of new physics not only beyond the Standard Model but also beyond its minimal extensions accounting for neutrino masses.

1.3 Its supersymmetric version

Because it solves the hierarchy problem, explains the breaking of the electroweak symmetry, achieves the unification of the gauge coupling constants, and provides a suitable candidate for the dark matter component of the Universe, low energy supersymmetry is the best motivated scenario for physics beyond the Standard Model.

Supersymmetric models are defined by a superpotential and a soft breaking Lagrangian. The superpotential determines the scalar interactions and Yukawa couplings as well as all particle masses in the supersymmetric limit. The soft breaking Lagrangian, on the other hand, parameterizes our ignorance of the mechanism of spontaneous supersymmetry breaking by introducing extra terms which explicitly break supersymmetry. Such terms consist of gaugino masses, scalar masses and scalar trilinear couplings.

These soft breaking terms are a new possible source of lepton flavor violation. As a result of GUT interactions, supersymmetry breaking, or Yukawa interactions at high energies, lepton flavor violating entries could have been generated in scalar masses and trilinear couplings. And since the LFV decays they give rise to are not suppressed by neutrino masses, their rates are expected to be much larger than in the non supersymmetric model.

The supersymmetric see-saw mechanism [6] is a minimal setup in which the Yukawa interactions induce lepton flavor violation in the soft Lagrangian. Even if the soft terms are assumed to be flavor blind at the GUT scale (as in mSUGRA models), renormalization group effects between the GUT and the right handed neutrino scale transmit the violation of lepton flavor from the neutrino Yukawa couplings to the left handed slepton mass matrix. At low energies, those matrix elements manifest themselves in LFV decays.

In the MSSM with right handed neutrinos the leptonic part of the superpotential is given by

$$W_l = e_R^T \mathbf{Y}_e L H_d + \nu_R^T \mathbf{Y}_\nu L H_u - \frac{1}{2}\nu_R^T \mathbf{M_R} \nu_R, \tag{1.9}$$

where L, e_R and ν_R denote respectively the lepton doublet, the right-handed charged lepton, and the right-handed neutrino; H_u and H_d are the two Higgs doublets needed in the MSSM. We will always work in the basis in which $\mathbf{M_R}$ and $\mathbf{Y}_e$ are diagonal. Consequently, all the information about the lepton flavor will be contained in $\mathbf{Y}_\nu$.

C.E.Y.

The relevant part of the soft breaking Lagrangian is

$$\begin{aligned} -\mathscr{L}_{soft} &= (\mathbf{m}^2_{\tilde{L}})_{ij}\tilde{L}^\dagger_i\tilde{L}_j + (\mathbf{m}^2_{\tilde{e}})_{ij}\tilde{e}^*_{Ri}\tilde{e}_{Rj} + (\mathbf{m}^2_{\tilde{\nu}})_{ij}\tilde{\nu}^*_{Ri}\tilde{\nu}_{Rj} \\ &+ \left(\mathbf{A}^e_{ij}H_d\tilde{e}^*_{Ri}\tilde{L}_j + \mathbf{A}^\nu_{ij}H_u\tilde{\nu}^*_{Ri}\tilde{L}_j + h.c.\right) \\ &+ m^2_{H_d}H^\dagger_dH_d + m^2_{H_u}H^\dagger_uH_u + (B\mu H_dH_u + h.c.) \\ &+ \frac{1}{2}M_1\tilde{B}\tilde{B} + \frac{1}{2}M_2\tilde{W}\tilde{W} + \frac{1}{2}M_3\tilde{g}\tilde{g}. \end{aligned} \tag{1.10}$$

However, due to the large number of free parameters it introduces, this generic soft breaking Lagrangian is not suitable for phenomenological analysis. The usual way of studying supersymmetric effects is to assume that the soft terms take on simplified forms at a certain high energy scale.

Minimal supergravity (mSUGRA) models, for instance, are defined in terms of only four continuous parameters and one sign

$$M_{1/2}, \quad m_0, \quad A_0, \quad \tan\beta, \quad \text{sign } \mu, \tag{1.11}$$

which determine the whole set of soft breaking terms at the GUT scale through the following relations

$$(\mathbf{m}^2_{\tilde{L}})_{ij} = (\mathbf{m}^2_{\tilde{e}})_{ij} = (\mathbf{m}^2_{\tilde{\nu}})_{ij} = \cdots = \delta_{ij}m_0^2\,, \tag{1.12}$$

$$\tilde{m}^2_{H_d} = \tilde{m}^2_{H_u} = m_0^2\,, \tag{1.13}$$

$$M_i = M_{1/2}\,, \tag{1.14}$$

$$\mathbf{A}^\nu = \mathbf{Y}_\nu A_0, \quad \mathbf{A}^e = \mathbf{Y}_e A_0\,. \tag{1.15}$$

To obtain the supersymmetric spectrum at low energies, the MSSM renormalization group equations (A) must be run down with these boundary conditions.

C.E.Y.

As a consequence of the renormalization group evolution between the unification scale and the right-handed neutrino scale, the left-handed slepton mass matrix ($\mathbf{m}^2_{\tilde{L}}$) acquires lepton flavor violating entries. In the leading-logarithmic approximation such entries are given by

$$(\mathbf{m}^2_{\tilde{L}})_{ij} \approx -\frac{1}{16\pi^2}(6+2a_0^2)m_0^2\mathbf{Y}^\dagger_{\nu_{ik}} \log\frac{M_X}{M_{R_k}}\mathbf{Y}_{\nu_{kj}}. \tag{1.16}$$

Thus, in the supersymmetric version of the see-saw mechanism, lepton flavor violating effects are controlled by the neutrino Yukawa couplings. Unfortunately, they are not known. Because the available experimental data from oscillation experiments is sensitive to the Yukawas only through the neutrino mass matrix ($\mathbf{Y}_\nu^T\mathbf{M}_\mathbf{R}^{-1}\mathbf{Y}_\nu$), there is no a direct relation between LFV processes and neutrino masses and mixing.

This lack of knowledge of the neutrino Yukawa couplings that prevents us from computing eq (1.16) is the most pressing problem concerning lepton flavor violating decays. And it is a matter of principle. No other low energy measurements will give enough information to reconstruct the neutrino Yukawa couplings. Thus, contrary to other supersymmetric predictions like $b\rightarrow s\gamma$, $(g-2)_\mu$, or the neutralino relic abundance, the computation of lepton flavor violating decays requires additional assumptions.

Within $SO(10)$ theories, for instance, the neutrino Yukawa couplings are usually related – via the unified symmetry – to the up-type quark Yukawas (see section 3.1). Or, assuming a given right-handed neutrino spectrum, the see saw formula could be inverted to obtain the Yukawa couplings in terms of low energy data (see section 2.3). Though constrained by the non-

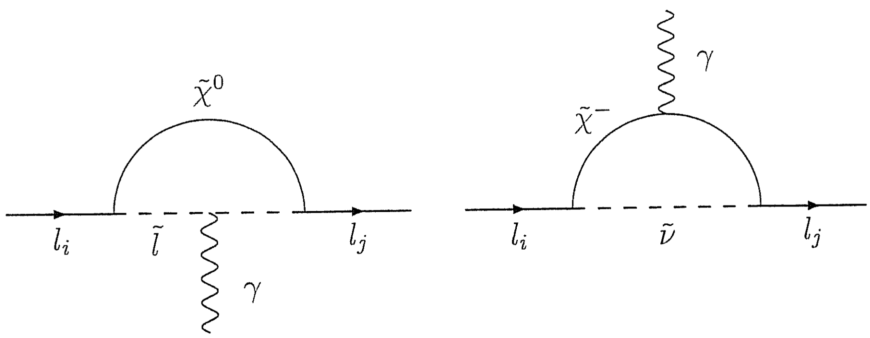

Figure 1.2: Diagrams for $l_i^- \to l_j^- \gamma$ in supersymmetry

observation of LFV decays, the off-diagonal elements in eq. (1.16) could also be considered as free parameters in the study of other supersymmetric effects (see chapter 4).

Anyhow, as long as the soft breaking Lagrangian violates the lepton flavor, LFV processes mediated by supersymmetric particles are allowed. In particular, the decay $\ell_j \to \ell_i \gamma$ receives contributions from two Feynman diagrams (fig 1.2): the chargino-sneutrino loop and the neutralino-charged slepton loop. In the appendix, the complete formulas for the decay rate and the branching ratio are provided. Throughout this thesis, we will be only concerned with the decays $\mu \to e\gamma$ and $\tau \to \mu\gamma$ and we will always use those formulas to compute their branching ratios.

Chapter 2

Three Common assumptions reviewed

2.1 The mass insertion

It is often stated that in the mass insertion approximation $BR(\ell_j \to \ell_i \gamma)$ is given by

$$BR(\ell_j \to \ell_i \gamma) \approx \frac{\alpha^3}{G_F^2} \frac{\left|(m_{\tilde{L}}^2)_{ji}\right|^2}{m_S^8} \tan^2 \beta, \qquad (2.1)$$

where m_S is a typical supersymmetric mass. Unfortunately, nobody knows what a typical supersymmetric mass is. Is it a neutralino or a chargino mass? Or it is the mass of the lightest sneutrino? Perhaps it is a properly weighted average of all them. But it matters. Because the dependence on m_S is so strong, without a prescription for it – in terms of physical parameters – the above formula is meaningless.

What is then the approximation behind eq. (2.1)? Is it really the mass insertion approximation? Actually no, as we now show.

The only source of lepton flavor violation in the minimal seesaw model are the off diagonal elements in the slepton mass matrix. The amplitudes of LFV processes, however, depend on such matrix elements in an entangled manner –only through the diagonalizing matrix. But, if the full diagonalization of mass matrices were replaced by a perturbative one around the identity, that dependence would become transparent. That is precisely what the mass insertion approximation does.

The prescription to extract from the general formulas the ones in terms of the off-diagonal elements, in the spirit of the mass insertion approximation, works as follows. Let us define

$$M^2 = diag(m_{0i}^2) + \Delta \tag{2.2}$$

$$= Z^\dagger diag(m_i^2) Z \tag{2.3}$$

where Z is some unitary matrix and Δ contains only off-diagonal elements. Then, for an arbitrary loop function f the following expansion holds

$$Z_{ki}^\dagger f(m_i^2) Z_{ij} = \delta_{kj} f(m_{0j}^2) + \Delta_{kj} F(m_{0k}^2, m_{oj}^2) + \mathcal{O}(\Delta^2/m_0^4) \tag{2.4}$$

with

$$F(x,y) = \frac{f(x) - f(y)}{x - y}\,. \tag{2.5}$$

The left-hand side in eq. (2.4) is a function of the diagonalizing matrix Z and the exact eigenvalues of M^2, whereas the right-hand side is written in terms of the diagonal and off-diagonal entries of that matrix. In fact, this expansion is equivalent to a first order diagonalization of M^2.

C.E.Y.

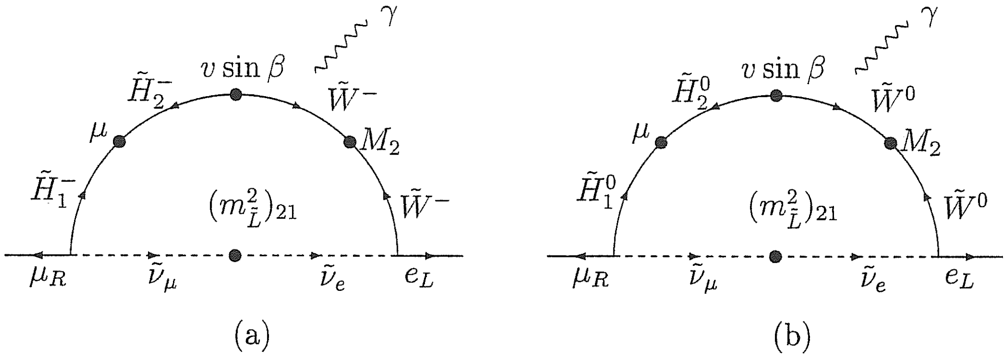

Figure 2.1: Dominant contributions to $\mu \to e\gamma$ in the mass insertion approximation. (a): the chargino contribution. (b): the neutralino contribution.

The mass insertion approximation is useful because it allows to detect the relevant parameters and to isolate the dominant diagrams. For example, the dominant contribution to $\mu \to e\gamma$ in the SUSY seesaw are given by the diagrams shown in fig 2.1. The mixing between the Higgsino and the gaugino ($\sim\ v\sin\beta$), and the Yukawa coupling of Higgsinos, leptons and sleptons ($\sim m/v\cos\beta$) give rise to a $\tan\beta$ enhanced amplitude.

Using eq. (2.4) for both the chargino and the sneutrino mass matrices, the dominant chargino contribution to the decay $\mu \to e\gamma$ turns out to be

$$A^c \approx \frac{\alpha_2}{4\pi\sqrt{2}}\frac{M_2\mu}{M_2^2-\mu^2}\frac{(m^2_{\tilde{L}})_{21}}{m^4_{\tilde{\nu}}}(g(x_{\mu\tilde{\nu}})-g(x_{2\tilde{\nu}}))\tan\beta\,. \tag{2.6}$$

Here, $m_{\tilde{\nu}} = m_{\tilde{\nu}_1} = m_{\tilde{\nu}_2}$, $x_{\mu\tilde{\nu}} = \mu^2/m^2_{\tilde{\nu}}$, $x_{2\tilde{\nu}} = M_2^2/m^2_{\tilde{\nu}}$, and $g(x)$ is a function defined in the appendix (eq C.16). The mass insertion approximation, therefore, does not introduce undefined parameters.

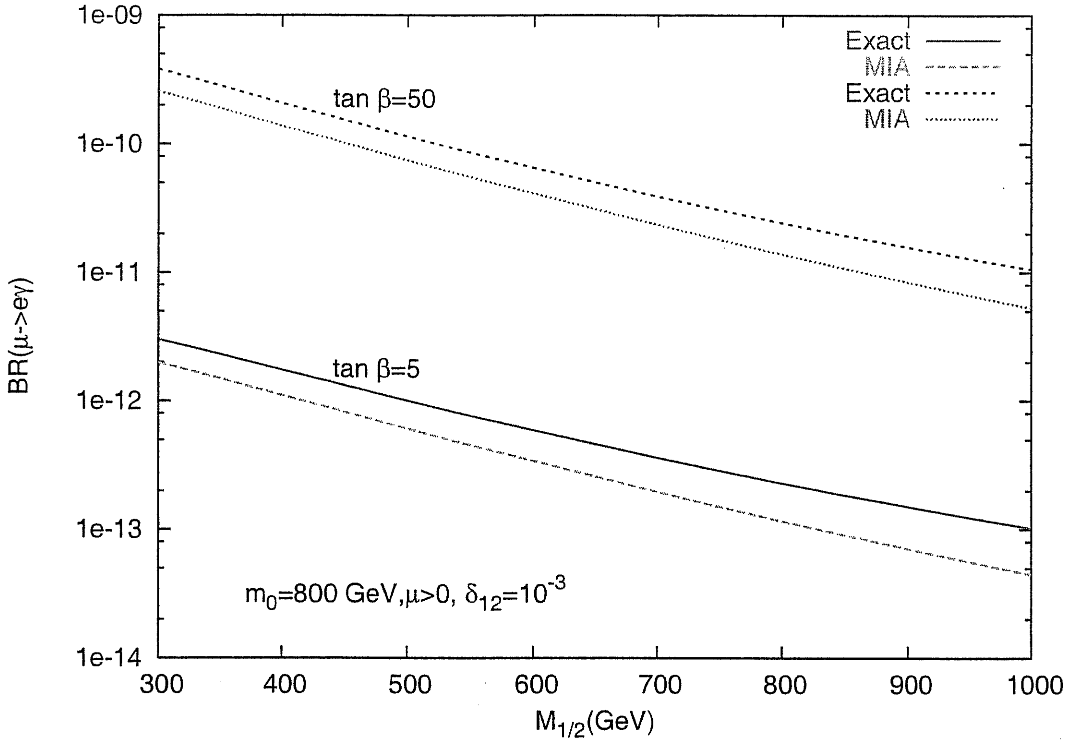

Figure 2.2: Comparison between the mass insertion approximation and the exact result.

An analogous expression can be obtained for the neutralino amplitude. However, it is usually a good approximation to assume that the chargino contribution is dominant. In fig 2.2 we show the exact result and the one obtained from eq. (2.6) for two different values of $\tan\beta$. The agreement is evident.

C.E.Y.

2.2 The leading-log

The renormalization group equation for the left-handed slepton mass matrix reads

$$\mu\frac{d}{d\mu}\left(m_{\tilde{L}}^2\right)_{ji} = \mu\frac{d}{d\mu}\left(m_{\tilde{L}}^2\right)_{ji}\Big|_{\rm MSSM} + \frac{1}{16\pi^2}\Big[\left(m_{\tilde{L}}^2\mathbf{Y}_\nu^\dagger\mathbf{Y}_\nu + \mathbf{Y}_\nu^\dagger\mathbf{Y}_\nu m_{\tilde{L}}^2\right)_{ji} + 2\left(\mathbf{Y}_\nu^\dagger m_{\tilde{\nu}}^2\mathbf{Y}_\nu + \tilde{m}_{H_u}^2\mathbf{Y}_\nu^\dagger\mathbf{Y}_\nu + A_\nu^\dagger A_\nu\right)_{ji}\Big] \quad . \tag{2.7}$$

The first term is the usual flavor diagonal contribution of the MSSM, whereas the second one is the source of lepton flavor violation in the SUSY seesaw model. Usually the leading logarithmic approximation

$$\left(m_{\tilde{L}}^2\right)_{ji} \approx -\frac{1}{8\pi^2}(3m_0^2 + A_0^2)\left(\mathbf{Y}_\nu^\dagger\mathbf{Y}_\nu\right)_{ji}\log\frac{M_{\rm GUT}}{M_R} \tag{2.8}$$

is used to compute LFV effects in models with mSUGRA boundary conditions. We want to assess the validity of this leading-log approximation. That is, we want to compare the exact results – eq.(2.7) – with the approximated ones – eq. (2.8) – and find the region in the supersymmetric parameter space where the approximation is not reliable.

For simplicity we will assume that right-handed neutrinos are degenerate and that light neutrinos are hierarchical, with $m_1 = 0.1m_2$ (see eq (1.3)). We will also fix θ_{13} to $\tan^2\theta_{13} = 0.01$ and set all CP phases to zero. The experimental input, therefore, consists of three neutrino masses and three mixing angles.

This data, however, is insufficient for fixing the neutrino Yukawa couplings needed in the evaluation of eqs (2.8) and (2.7). To do that, we rely on a best fit approach. At the GUT scale, neutrino Yukawa couplings are generated randomly and then run down to the right-handed neutrino scale, where the effective neutrino mass matrix is formed. This matrix is run down to the electroweak scale where it is compared against the experimental data. In order to find the best possible fit, we define a quantity, b.p.f. as

$$\text{b.p.f.} \equiv \sum \left[\ln \left(\frac{\langle f \rangle}{f_{\text{exp}}} \right) \right]^2 . \tag{2.9}$$

Here, $\langle f \rangle$ denotes the predicted masses and mixing angles for a given set of neutrino Yukawa couplings and f_{exp} denotes the corresponding experimental values. A matrix of neutrino Yukawa couplings is considered to be appropriate if b.p.f.$\leq 10^{-2}$.

With the neutrino Yukawa couplings thus determined, we compute the off-diagonal elements in the slepton mass matrix using eqs (2.8) and (2.7). Since BR($\ell_j \to \ell_i \gamma$) goes as $\mid (m_{\tilde{L}}^2)_{ji} \mid^2$ the meaningful quantity to be compared is the square of the ratio between the exact result and the leading log approximation. In fig 2.3, we show such ratio as a function of $M_{1/2}$ for $M_R = 10^{11}$GeV and different values of m_0. The trend is clear: for a fixed value of $M_{1/2}$, the smaller m_0, the larger the ratio; whereas for a fixed m_0, the larger $M_{1/2}$ the larger the ratio. And, at large $M_{1/2}$, the error induced in the computation of $BR(\mu \to e\gamma)$ by the use of the logarithmic approximation could amount to more than one order of magnitude.

The dependence of this ratio on M_R is illustrated in fig 2.4. It is apparent that the larger the value of M_R the larger the ratio. This behavior may seem puzzling at first for the approximation should be better the closer M_R is to

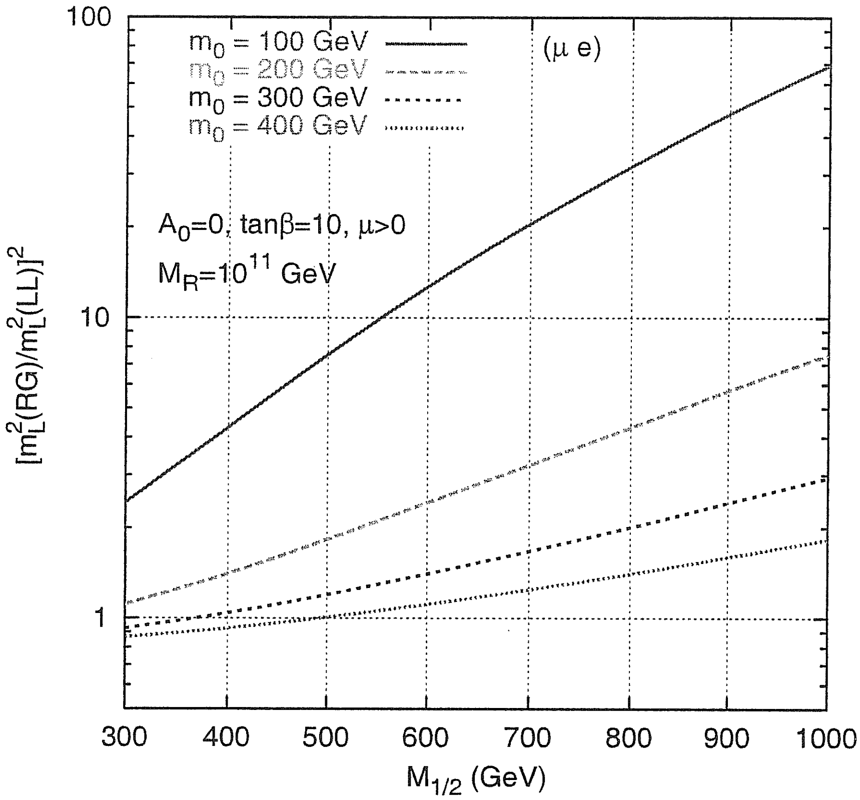

Figure 2.3: *The leading log approximation for different values of* m_0.

the GUT scale. However, owing to the seesaw formula, different values of M_R require different sets of neutrino Yukawa couplings. So, each line in fig 2.4 actually represents a different model. It is also clear from the figure that the ratio only differs significantly from 1 at large $M_{1/2}$.

The leading-log approximation, therefore, ceases to be valid in the region $M_{1/2} \gg m_0$.

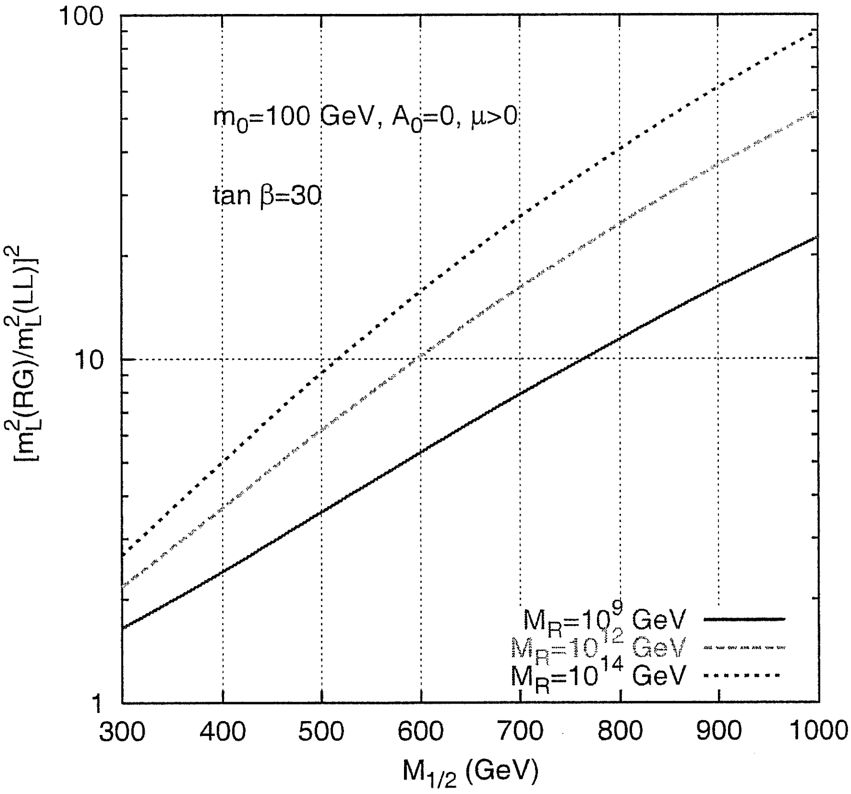

Figure 2.4: *The leading log approximation for different values of M_R.*

2.3 Real R

The see saw formula can be inverted to obtain the neutrino Yukawa couplings in terms of the right handed neutrino spectrum and neutrino masses and mixing angles, but at the price of introducing an orthogonal matrix **R** as

$$\mathbf{Y}_\nu = \frac{1}{v_u}\mathbf{M_R}^{1/2}\mathbf{R}m_\nu^{1/2}U^\dagger \, . \tag{2.10}$$

This useful parameterization uses as input the measured values of neutrino masses and mixing angles (m_ν, U) and clearly shows that they are not enough for reconstructing the neutrino Yukawa couplings.

Rates for LFV processes in SUSY will then depend on

$$\mathbf{Y}_\nu^\dagger \mathbf{Y}_\nu = \frac{1}{v_u^2} U m_\nu^{1/2} \mathbf{R}^\dagger \mathbf{M_R} \mathbf{R} m_\nu^{1/2} U^\dagger. \tag{2.11}$$

A particularly simple form is obtained if right-handed neutrinos are degenerate and $\mathbf{R}$ is real:

$$\mathbf{Y}_\nu^\dagger \mathbf{Y}_\nu = \frac{M_R}{v_u^2} U m_\nu U^\dagger. \tag{2.12}$$

Indeed, the mass of the right-handed neutrinos is practically the only unknown in this expression. BR($\mu \to e\gamma$) will be proportional to

$$\left(\mathbf{Y}_\nu^\dagger \mathbf{Y}_\nu\right)_{21} = \frac{M_R}{v_u^2} \left[U_{\mu 2} U_{e2}^* (m_{\nu 2} - m_{\nu 1}) + U_{\mu 3} U_{e3}^* (m_{\nu 3} - m_{\nu 1})\right]. \tag{2.13}$$

In different studies this equation was used to compute BR($\mu \to e\gamma$) and to obtain the viable supersymmetric parameter space. We found, however, that if $\mathbf{R}$ is complex and neutrinos are quasi degenerate, $\left(\mathbf{Y}_\nu^\dagger \mathbf{Y}_\nu\right)_{21}$ is generally much larger than expected from eq.(2.13).

The reason for this enhancement is twofold. First, since eq. (2.13) depends on mass differences, the term proportional to m_ν – the leading one – cancels out. Second, the dominant mass difference ($\propto \Delta m^2_{atm}$) is multiplied by the mixing factor U_{e3}, which is small and might even be zero. Thus, instead of the natural estimate $M_R m_\nu / v_u^2$, $\left(\mathbf{Y}_\nu^\dagger \mathbf{Y}_\nu\right)_{21}$ will be suppressed to $M_R \Delta m^2_{solar} / (v_u^2 m_\nu)$ for small s_{13}. These suppression effects are avoided if $\mathbf{R}$ is complex, giving rise to enhanced rates.

A complex $\mathbf{R}$ matrix is not only natural but also necessary if the baryon asymmetry of the Universe is to be explained through leptogenesis. In leptogenesis, the CP violating decays of right-handed neutrinos produce a lepton asymmetry that is partially reprocessed by sphaleron processes into a baryon asymmetry. And the sources of CP violation are precisely the phases in $\mathbf{R}$; if it is real leptogenesis does not work.

The complex orthogonal matrix $\mathbf{R}$ can be written as

$$\mathbf{R} = e^{i\mathbf{A}}\mathbf{O}, \tag{2.14}$$

with $\mathbf{A}$ and $\mathbf{O}$ real matrices. The orthogonality of $\mathbf{R}$ implies that $\mathbf{O}$ is orthogonal and $\mathbf{A}$ antisymmetric. Since our main concern is the effect of a complex $\mathbf{R}$, we will assume for simplicity that $\mathbf{O} = 1$.

The off-diagonal elements in the slepton mass matrix will then be proportional to

$$\left(\mathbf{Y}_\nu^\dagger \mathbf{Y}_\nu\right)_{ij} \simeq \frac{1}{v_u^2} M_R m_\nu (U e^{i2\mathbf{A}} U^\dagger)_{ij}\,. \tag{2.15}$$

The exponential factor is easily computed. If we write

$$\mathbf{A} = \begin{pmatrix} 0 & a & b \\ -a & 0 & c \\ -b & -c & 0 \end{pmatrix}, \tag{2.16}$$

then, $e^{i\mathbf{A}}$ can be calculated explicitly to obtain

$$e^{i\mathbf{A}} = 1 - \frac{\cosh r - 1}{r^2}\mathbf{A}^2 + i\frac{\sinh r}{r}\mathbf{A} \tag{2.17}$$

with $r = \sqrt{a^2 + b^2 + c^2}$.

We claim that $(\mathbf{Y}_\nu^\dagger \mathbf{Y}_\nu)_{21}$ for $\mathbf{R}$ complex is typically much larger than it is for $\mathbf{R}$ real. By typically we mean when a, b, c are not too small. This fact is illustrated in fig 2.5, when we show a scatter plot of the quantity

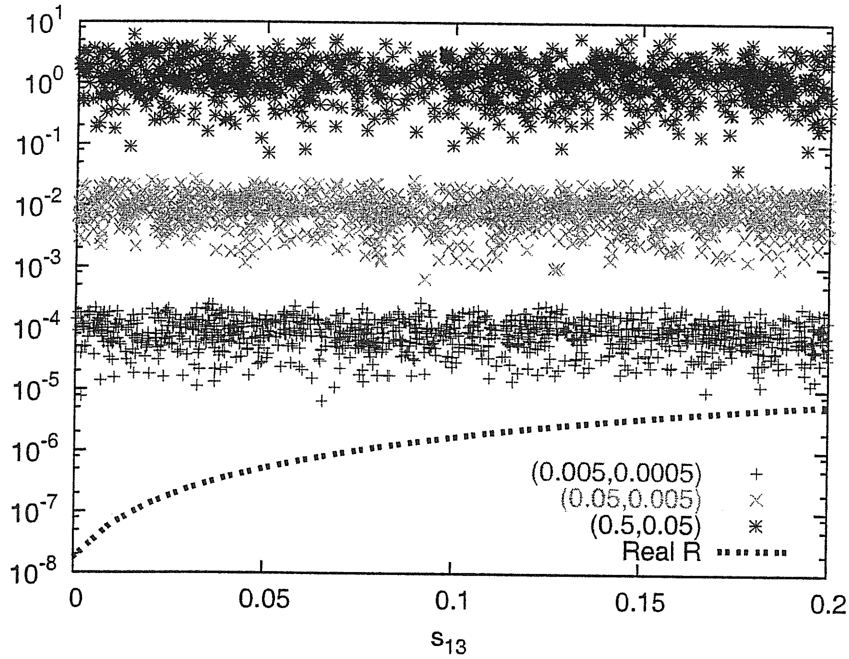

Figure 2.5: $\left|v_u^2(Y_\nu^\dagger Y_\nu)_{12}/(M_R m_\nu)\right|^2$ *for R real (black line) and R complex (points). The parameters* a, b, c *defining R were generated randomly in the intervals* $(0.5, 0.05)$ *for the* $*$ *points,* $(0.05, 0.005)$ *for the* $\times$ *points, and* $(0.005, 0.0005)$ *for* $+$ *points.*

$v_u^4|(\mathbf{Y}_\nu^\dagger \mathbf{Y}_\nu)_{21}|^2/(M_R^2 m_\nu^2)$ as a function of s_{13}. The black line is the prediction for $\mathbf{R}$ real. As expected from eq. (2.13), it is an increasing function of s_{13}. The different type of points, on the other hand, indicate the diverse ranges in which a, b, c are assumed to vary randomly. The convention is

$*$ for a, b, c in the interval $(0.5, 0.05)$

$\times$ for a, b, c in the interval $(0.05, 0.005)$

$+$ for a, b, c in the interval $(0.005, 0.0005)$.

If a, b, c are of order 10^{-1} (*), the difference between the real and the complex **R** amounts to five orders of magnitude for $s_{13} = 0.2$ and reaches eight orders of magnitude for $s_{13} = 0.0$. Such difference get reduced for smaller values of a, b, c but is significant – up to four orders of magnitude – even when they are of order 10^{-3} (+). Thus, **R** real is not always a good approximation and much larger values of $BR(\mu \to e\gamma)$ are usually obtained for **R** complex.

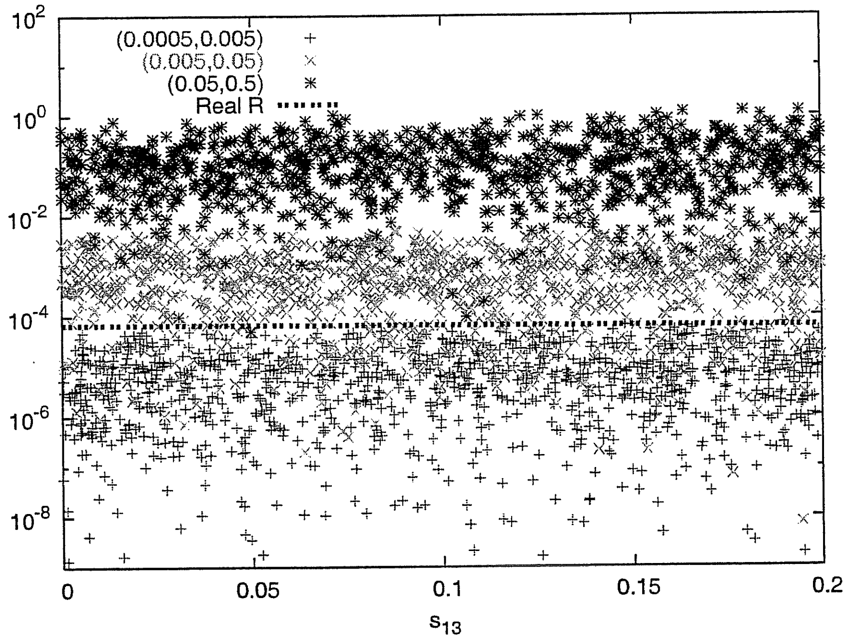

Figure 2.6: *The same as in fig. 2.5 but for the matrix element* (3, 2).

For the decay $\tau \to \mu\gamma$ the situation is quite different (fig 2.6). First of all, for **R** real (the line) the dependence with s_{13} is very weak –unnoticeable. Second, the enhancement not only is much smaller but disappears and becomes a suppression for $a, b, c \sim 10^{-3}$. $\tau \to \mu\gamma$ is therefore less sensitive than $\mu \to e\gamma$ to the effects of a complex **R** matrix.

C.E.Y.

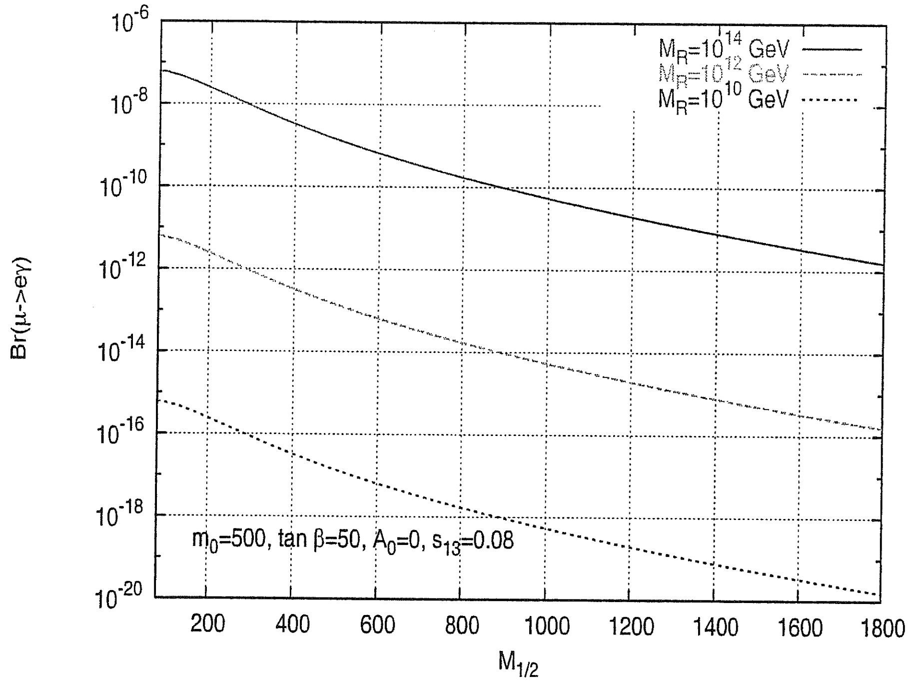

Figure 2.7: *$BR(\mu \to e\gamma)$ as a function of $M_{1/2}$ for $m_0 = 800\,GeV$, $\tan\beta = 50$ and R real for different values of the right-handed neutrino mass.*

Suppose now that you find out that a, b, c must be of order 10^{-1}, so that a strong enhancement in $BR(\mu \to e\gamma)$ takes place. Does this enhancement rule the model out? Actually not because $BR(\mu \to e\gamma)$ depends also on the mass of the right-handed neutrino. And that dependence ($\propto M_R^2$) is so strong (fig 2.7) that meaningful constraints can be obtained only if M_R is known. Indeed, even an enhancement of eight orders of magnitude can be compensated with a four orders of magnitude smaller right-handed neutrino mass. Nonetheless, $M_R \geq 10^{12}$ GeV would certainly be rule out.

C.E.Y.

Chapter 3

Lepton flavor violation in an SO(10) model

3.1 The model

Grand Unified Theories (GUTs) have the potential to unify into a single, comprehensive and predictive framework the diverse set of particle representations and parameters of the Standard Model. They might explain the quantum numbers of fermions, the origin of fermion masses, and the quantization of the electric charge. And the apparent gauge coupling unification of the minimal supersymmetric standard model provides evidence in favor of a SUSY GUT.

Among the different Lie groups that contain $SU(3) \times SU(2) \times U(1)$ as a subgroup, SO(10) is the smallest one which can accommodate an entire family of the Standard Model into a single anomaly-free irreducible representation. That representation is 16-dimensional and consists of the SM matter fields plus the right-handed neutrino. In $SO(10)$, therefore, neutrino masses are naturally generated. Additionally, the lifetime of the proton in $SO(10)$ models is long enough to be compatible with present experimental bounds. For all these reasons, $SO(10)$ is an attractive unification group.

Once $SO(10)$ is fixed as the gauge group, many choices are left for the Higgs representations. The most common include 10, 45, 54, 120, $\overline{126}$, 126 and 210. They play an essential role in the spontaneous breaking of the $SO(10)$ symmetry (45, 54) and in the generation of fermion masses (10, 126, 120).

A certain class of $SO(10)$ models predicts a large mixing in the neutrino Yukawa couplings. If, for instance, the down-quark sector couples to a combination of symmetric and antisymmetric Higgs representations (Φ), the resulting mass matrix is not symmetric and the small CKM mixing typical of symmetric representations can be avoided.

Let us consider the following superpotential

$$W_{SO(10)} = \frac{1}{2}\,\mathbf{Y}^{u,\nu}_{ij}\;16_i\;16_j 10^u + \frac{1}{2}\,\mathbf{Y}^{d,e}_{ij}\;16_i\;16_j\Phi + \frac{1}{2}\,\mathbf{Y}^{R}_{ij}\;16_i\;16_j 126 \tag{3.1}$$

and assume that the 126 generates only the right-handed neutrino mass matrix. $\mathbf{Y}^d$, being non-symmetric, is diagonalized by two different matrices. If they are precisely the CKM and the PMNS mixing matrices, we may write

$$V^T_{CKM}\,\mathbf{Y}^d\,U^T_{PMNS} = \mathbf{Y}^d_{diag}. \tag{3.2}$$

Thus, in the basis where the down sector is diagonal, a CKM mixing is

C.E.Y.

generated in the quark sector and a PMNS mixing is generated in $\mathbf{Y}_\nu$ [7]:

$$\mathbf{Y}_u = V_{CKM} \mathbf{Y}_u^{diag} V_{CKM}^T \tag{3.3}$$

$$\mathbf{Y}_\nu = U_{PMNS} \, \mathbf{Y}_u^{diag}. \tag{3.4}$$

So, the neutrino Yukawa coupling is determined in terms of the up-quark Yukawas and the neutrino mixing matrix.

The right-handed neutrino mass matrix, on the other hand, is obtained as an output from the see-saw formula:

$$\mathbf{M_R} = \mathrm{Diag}\left\{ \frac{m_u^2}{m_{\nu_1}}, \frac{m_c^2}{m_{\nu_2}}, \frac{m_t^2}{m_{\nu_3}} \right\}. \tag{3.5}$$

We will assume that the spectrum of light neutrinos is hierarchical, eq(1.3), and consequently $M_{R_3} \approx 10^{14}$GeV.

The off-diagonal elements of the left-handed slepton mass matrix can therefore be computed through eqs (3.3) and (3.5) in terms of the PMNS matrix, neutrino masses, and the up-type Yukawa couplings. In particular, the (2, 1) and (3, 2) elements of such matrix – relevant for $\mu \to e\gamma$ and $\tau \to \mu\gamma$ – are given by

$$(m_{\tilde{L}}^2)_{21} \approx -\frac{3m_0^2 + A_0^2}{8\pi^2} Y_t^2 U_{e3} U_{\mu 3} \ln \frac{M_{GUT}}{M_{R_3}} + \mathcal{O}(Y_2^\nu)^2, \tag{3.6}$$

$$(m_{\tilde{L}}^2)_{32} \approx -\frac{3m_0^2 + A_0^2}{8\pi^2} Y_t^2 U_{\mu 3} U_{\tau 3} \ln \frac{M_{GUT}}{M_{R_3}} + \mathcal{O}(Y_2^\nu)^2. \tag{3.7}$$

Thus, within this framework $\mu \to e$ transitions depend on the unknown matrix element U_{e3}.

In the following we will use these formulas to compute $BR(\mu \to e\gamma)$ and $BR(\tau \to \mu\gamma)$. We want to investigate the impact of their present and future experimental limits on the mSUGRA parameter space and to confront indirect searches through LFV decays against direct searches at the LHC.

3.2 Usual constraints on the mSUGRA parameter space

A variety of low energy measurements have been used to obtain constraints on the parameter space of mSUGRA models. Next, we will briefly reviewed the most relevant of those constraints.

3.2.1 Dark matter

The MSSM provides a unique dark matter candidate: the lightest neutralino. Dark matter bounds on the susy parameter space derive from the requirement that the neutralino relic abundance fall within the cosmologically preferred range. The recent data from WMAP increased to an unprecedented degree the accuracy in the determination of the dark matter content of the Universe. They indicate that [8]

$$0.09 \leq \Omega_{CDM} h^2 \leq 0.13 \qquad (3.8)$$

at the 95% confidence level. Since the lower limit can be evaded if dark matter is made up not solely of neutralinos, we will only require that $\Omega_\chi h^2 \leq 0.13$. This bound on SUSY models usually translates into an upper limit on the neutralino mass.

In mSUGRA models the dark matter constraint is particularly strong. In fact, because the lightest neutralino is normally a pure bino, the $\chi\chi$ annihilation cross section is small and the resulting Ω_χ typically exceeds the bound. Specific suppression mechanisms are then needed to achieve a neutralino relic density in the correct range.

Indeed, the WMAP upper bound on the relic density is fulfilled only in the three following regions:

- *The Stau Coannihilation Region:* In this region the lightest stau and the lightest neutralino are quasi degenerate ($m_\chi \approx m_{\tilde{\tau}}$) and efficient stau-stau as well as stau-neutralino (co-)annihilations suppress the thermal neutralino relic abundance below the WMAP bound.

  Since the condition $m_\chi \approx m_{\tilde{\tau}}$ can be easily satisfied, a coannihilation region exist for every value of $\tan\beta$ and independently of sign μ.

- *Funnel Region:* In this region the bino-bino annihilation cross section is greatly enhanced through resonant s-channel exchange of the heavy neutral Higgs A. The condition required for the resonant enhancement is $2m_\chi \approx m_A$, which may be fulfilled only for large $\tan\beta$ and $\mu < 0$.

- *Focus point or Hyperbolic Branch Region:* In this region m_0 is very large, yielding a *low* value of μ that translates into a non-negligible higgsino fraction in the lightest neutralino. Being partially higgsino, the neutralino has a larger annihilation cross section that suppresses its relic density. The focus point lies close to the region where radiative electroweak symmetry breaking is not valid, and so is relatively unstable numerically.

3.2.2 $b \to s\gamma$

A weighted averaging of the branching fraction $BF(b \to s\gamma)$ as measured by the BELLE, ALEPH, and CLEO collaborations leads to the bound [9]

$$2 \times 10^{-4} \leq BR(b \to s\gamma) \leq 4.6 \times 10^{-4} \tag{3.9}$$

at the 95% confidence level.

In the standard model the decay $b \to s\gamma$ proceeds through the tW loop and the prediction for its branching ($\sim 3.2 \times 10^{-4}$) is in good agreement with eq (3.9). In mSUGRA models, additional contributions to $b \to s\gamma$ from the $\tilde{t}\tilde{W}$ and tH^+ loops potentially destroy this agreement with the experimental results. Therefore, the SUSY spectrum must be heavy enough to suppress these new contributions within the experimental limits.

The sign of the supersymmetric contribution to $b \to s\gamma$ is anticorrelated, in mSUGRA models, with the sign of μ. For $\mu > 0$, SUSY contributions are negative and it is the lower limit on $BR(b \to s\gamma)$ that gives a constraint; whereas for $\mu < 0$, they are positive and it is the upper bound that matters. In both cases, light superpartners are disfavored.

C.E.Y.

3.2.3 Other constraints

The muon anomalous magnetic moment, $a_\mu = (g-2)_\mu/2$, has been measured recently by the E821 experiment: $a_\mu = 11659204(7)(5) \times 10^{-10}$. The most challenging parts of the SM calculation are the hadronic light-by-light and vacuum polarization contributions. At present these results are in dispute and thus different results for the deviation from the SM (δa_μ) have been published. If data from $e^+e^- \to hadrons$ is used to determine the hadronic vacuum polarization then [9]:

$$\delta a_\mu = (27.1 \pm 9.4) \times 10^{-10} \quad [10] \tag{3.10}$$

$$\delta a_\mu = (31.7 \pm 9.5) \times 10^{-10} \quad [11] \tag{3.11}$$

If, instead, the τ decay data is used, the deviation is smaller:

$$\delta a_\mu = (12.4 \pm 8.3) \times 10^{-10} \quad [10]\,. \tag{3.12}$$

Due to these uncertainties δa_μ is not a reliable constraint.

The unsuccessful searches for the Higgs boson and supersymmetric particles at LEP imply that $m_\chi > 100$ GeV and $m_h > 114$ GeV. In mSUGRA, the former condition translates into a lower bound for the neutralino mass $m_\chi > 50$ GeV whereas the latter rules out $\tan\beta \lesssim 5$.

3.3 Constraints from $\mu \to e\gamma$ and $\tau \to \mu\gamma$

The constraints considered in the previous section are generic; they do not refer to the particular $SO(10)$ model introduced in sec 3.1. What is specific

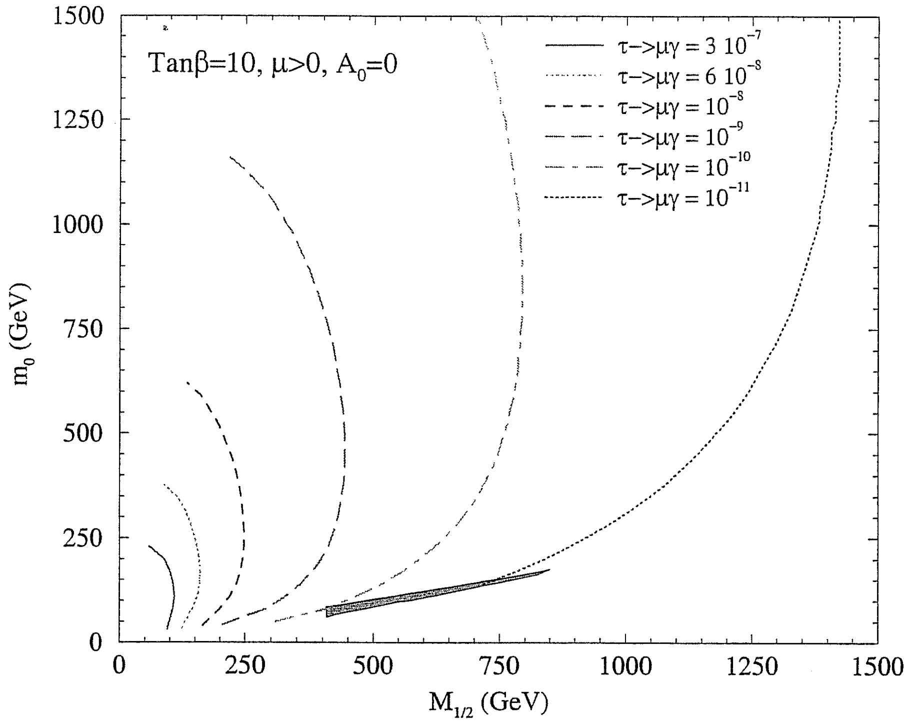

Figure 3.1: The parameter space of mSUGRA models (at $\tan\beta = 10$, $A_0 = 0$,$\mu > 0$) and different isolevels of $BR(\tau \to \mu\gamma)$.

about such model is that LFV effects are predicted in terms of low energy quantities. $\mu \to e\gamma$ and $\tau \to \mu\gamma$ therefore constitute real tests of that particular model.

The parameter space of mSUGRA models is conveniently displayed in a $(m_0, M_{1/2})$ plane for fixed values of the remaining parameters – $\tan\beta$, A_0 and signμ. In fig 3.1 we show the viable parameter space (the green zone) and isolevel curves of $BR(\tau \to \mu\gamma)$ for $\tan\beta = 10$, $A_0 = 0$, and $\mu > 0$. We see that the present experimental limit on $\tau \to \mu\gamma$ already starts probing

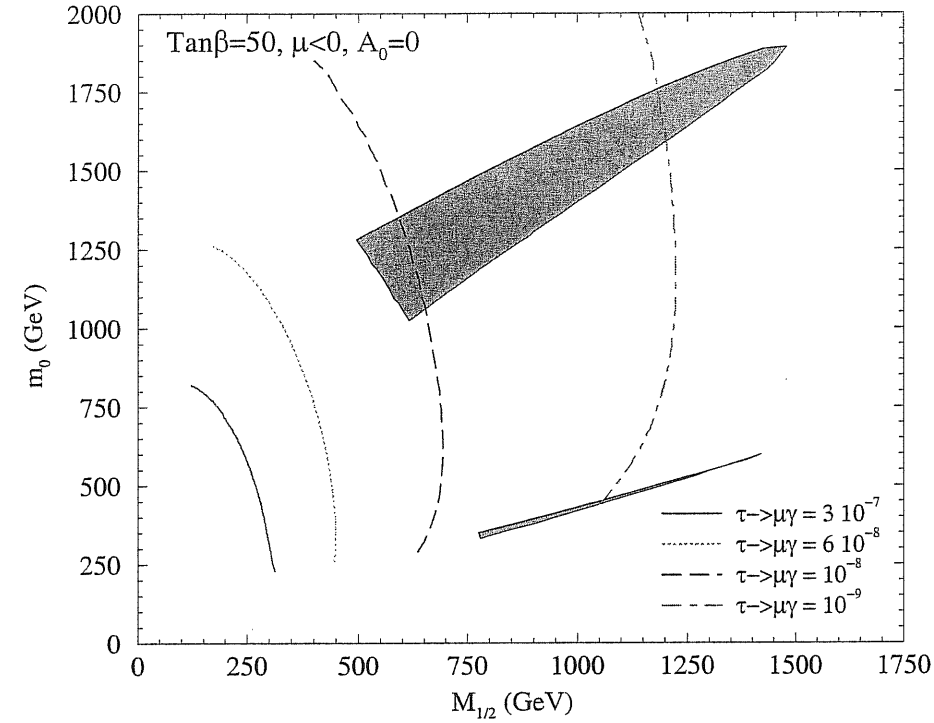

Figure 3.2: The parameter space of mSUGRA models (at $\tan\beta = 50$, $A_0 = 0$,$\mu < 0$) and different isolevels of $BR(\tau \to \mu\gamma)$.

the region of the parameter space at low m_0 and low $M_{1/2}$, which is likely to be tested at the Tevatron. However, what really matters is the prediction for $BR(\tau \to \mu\gamma)$ within the coannihilation region, and this value ($\lesssim 10^{-10}$) is well beyond the sensitivity of planned experiments. Therefore, for this set of parameters and in particular for this value of $\tan\beta$, $\tau \to \mu\gamma$ does not give any meaningful constraint on mSUGRA models.

The large $\tan\beta$ region, where the decay rate ($\propto \tan^2\beta$) is much larger offer better perspectives.. In fig 3.2, isolevel curves of $BR(\tau \to \mu\gamma)$ for

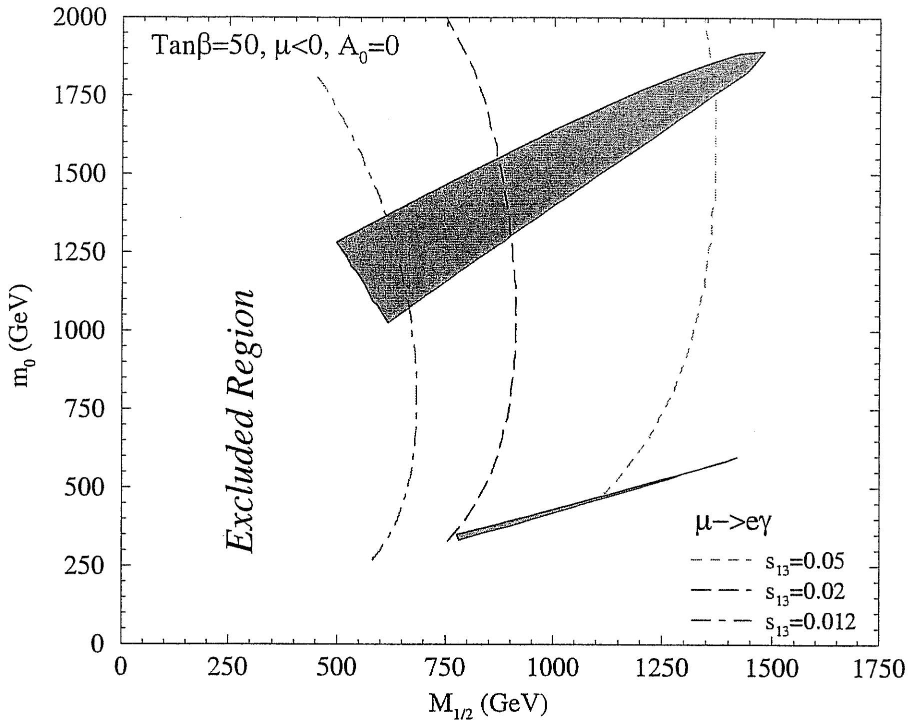

Figure 3.3: Exclusion plot of $\mu \to e\gamma$ for $\tan\beta = 50$

$\tan\beta = 50$, $A_0 = 0$, and $\mu < 0$ are shown. Since $\mu < 0$ and $\tan\beta$ is large, the A-pole funnel region (the bigger green patch) is also open. We see that values of m_0 up to 800 GeV and $M_{1/2}$ up to 300 GeV are excluded by the present experimental bound on $BR(\tau \to \mu\gamma)$. The intersection of the isolevel curves with the coannihilation region and the funnel takes place for $BR(\tau \to \mu\gamma) \approx 10^{-8}$, below the present limit but within the reach of proposed experiments.

Since the amplitude of $\mu \to e\gamma$ is U_{e3} dependent, we prefer to plot isolevels corresponding to its experimental limit for several values of U_{e3} (fig 3.3), so that the region at smaller m_0 and $M_{1/2}$ of a given isolevel is excluded. The results are remarkable. Taking $s_{13} = 0.2$, the present experimental upper bound, would rule out the whole parameter space. This fact can be interpreted either as a negative result for a large s_{13} or for a large value of $\tan\beta$. In both cases, with relevant implications for supersymmetric seesaw models. In the figure, we show isolevels corresponding to $s_{13} = 0.05, 0.02, 0.012$. Even such a small value as $s_{13} = 0.02$ can still exclude $M_{1/2} < 750\,\text{GeV}$ for any value of m_0.

In conclusion, $\tau \to \mu\gamma$ might turn into a relevant constraint on the SUSY parameter space provided that $\tan\beta$ be large and the experimental sensitivity reach BR($\tau \to \mu\gamma$)$\approx 10^{-8}$. $\mu \to e\gamma$ gives a much stronger bound and already excludes large values of s_{13} and significant portions of the parameter space. And, if s_{13} were known, $\mu \to e\gamma$ would emerge as the most important constraint on the supersymmetric parameter space of this model.

3.4 Discovering supersymmetry: $\mu \to e\gamma$ versus the LHC

The LHC is being built with the goal of discovering the Higgs boson and superpartners. Yet, even if superpartners are out there, they could escape detection at the LHC and, for a long time, leave $\mu \to e\gamma$ as the only evidence of their existence. The possibilities for that to happen are small in the coannihilation region, moderate in the funnel region and big in the focus

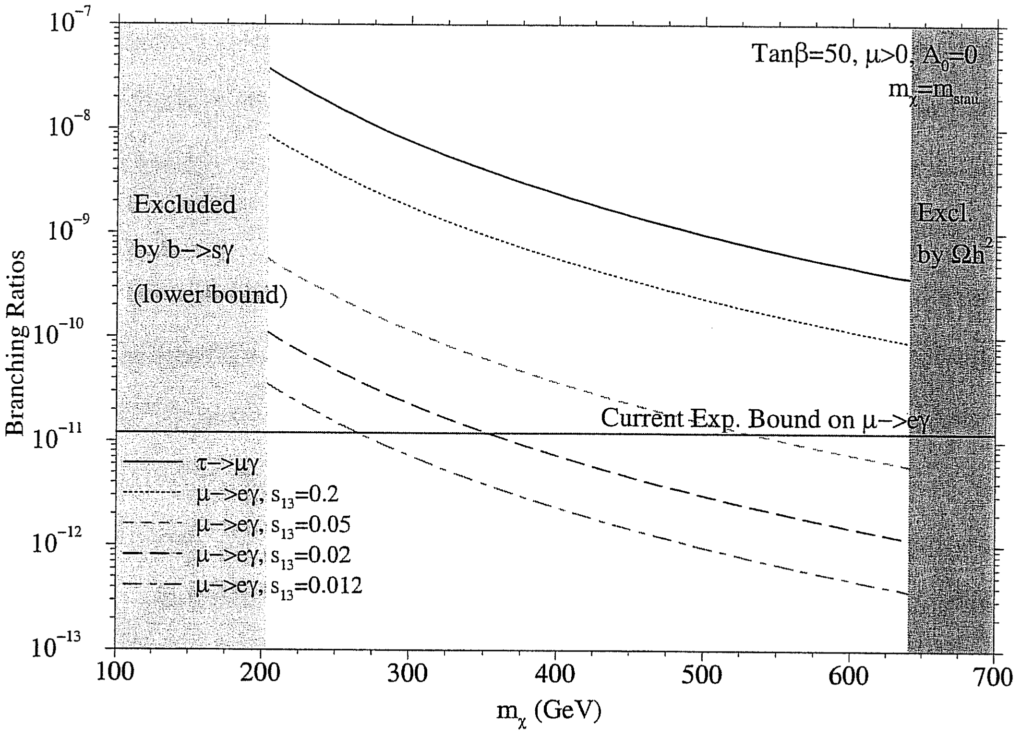

Figure 3.4: $BR(\mu \to e\gamma)$ and $BR(\tau \to \mu\gamma)$ as a function of the neutralino mass along the coannihilation strip ($m_\chi = m_{\tilde{\tau}}$). Constraints from $b \to s\gamma$ and the relic density rule out the extreme

C.E.Y.

point.

Indeed, the coannihilation strips will be almost completely within the reach of the LHC, and so $\mu \to e\gamma$ can hardly compete against direct searches. In fig 3.4 we show, as a function of the neutralino mass, typical predictions for $\mu \to e\gamma$ and $\tau \to \mu\gamma$ along the $m_\chi = m_{stau}$ line at $\tan\beta = 50$. The perspectives for $\tau \to \mu\gamma$ are not promising, for future experiments will be sensitive only to the low neutralino mass region, $m_\chi \approx 200$GeV. On the contrary, the current experimental bound on $BR(\mu \to e\gamma)$ already puts severe constraints on s_{13}, and future bounds will rule out $s_{13} \geq 0.01$.

In the funnel region the reach of the LHC will be limited to $m_\chi \leq 500$GeV (fig 3.5) and therefore $\mu \to e\gamma$ can actually challenge the LHC in the discovery road towards supersymmetry. As usual, the dependence with s_{13} is critical and is better illustrated in fig 3.6. From these two figures we infer that if $m_\chi \geq 500$GeV and $s_{13} > 10^{-2}$ supersymmetry will not be observed at the LHC but will be indirectly detected through $\mu \to e\gamma$ in planned experiments.

In the focus point region the reach of the LHC is very limited ($m_\chi \leq 200$GeV) due to the large values of m_0 and $M_{1/2}$ yielding heavy gluinos and squarks. BR($\mu \to e\gamma$), on the other hand, may be within future experimental sensitivity even for neutralino masses in the multi-TeV region (fig 3.4). Thus, in the focus point region, $\mu \to e\gamma$ overwhelmingly defeats the LHC in the search for supersymmetry.

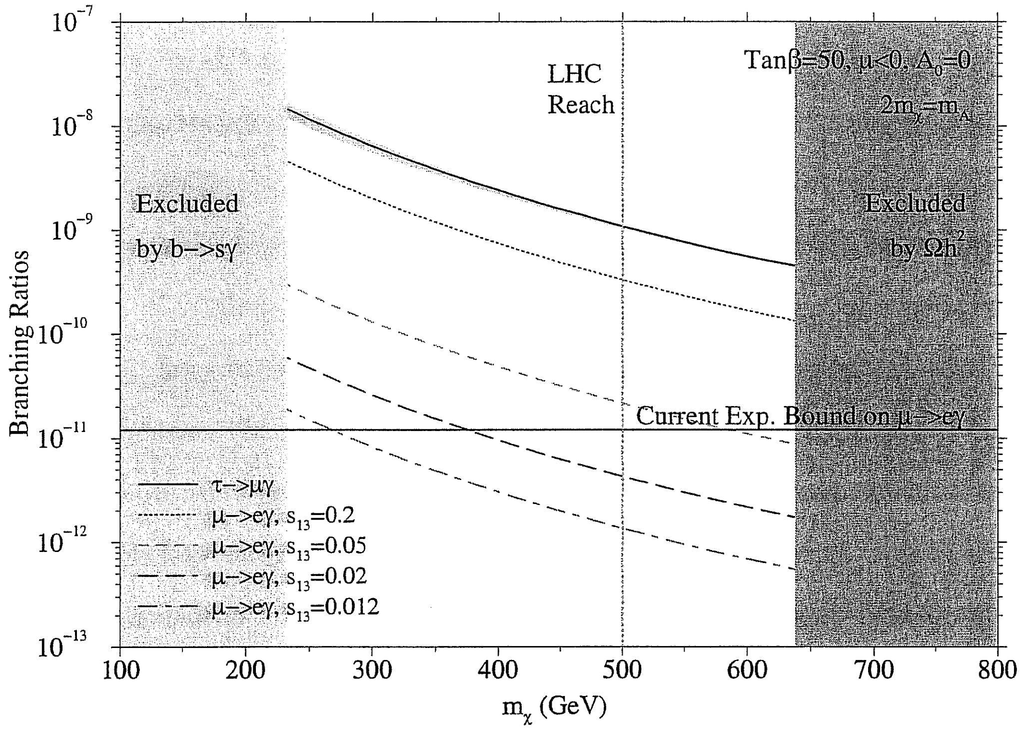

Figure 3.5: $BR(\mu \to e\gamma)$ and $BR(\tau \to \mu\gamma)$ as a function of the neutralino mass along the central part of the funnel region. Points in the yellow region are excluded by the $b \to s\gamma$ bound whereas those in the green region are ruled out by the dark matter constraint.

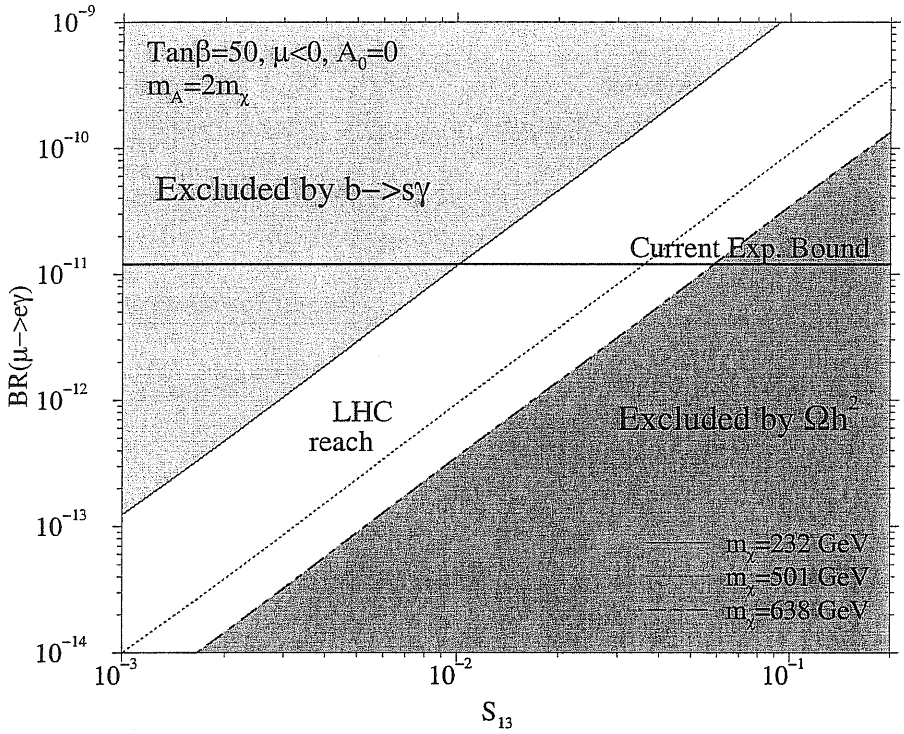

Figure 3.6: The dependence of $BR(\mu \to e\gamma)$ on s_{13} along the central part of the funnel ($2m_\chi = m_A$) for $\tan\beta = 50$, $\mu < 0$ and $A_0 = 0$. The upper region (in yellow) is ruled out by the $b \to s\gamma$ bound whereas the lower region (in green) is ruled out by the dark matter constraint.

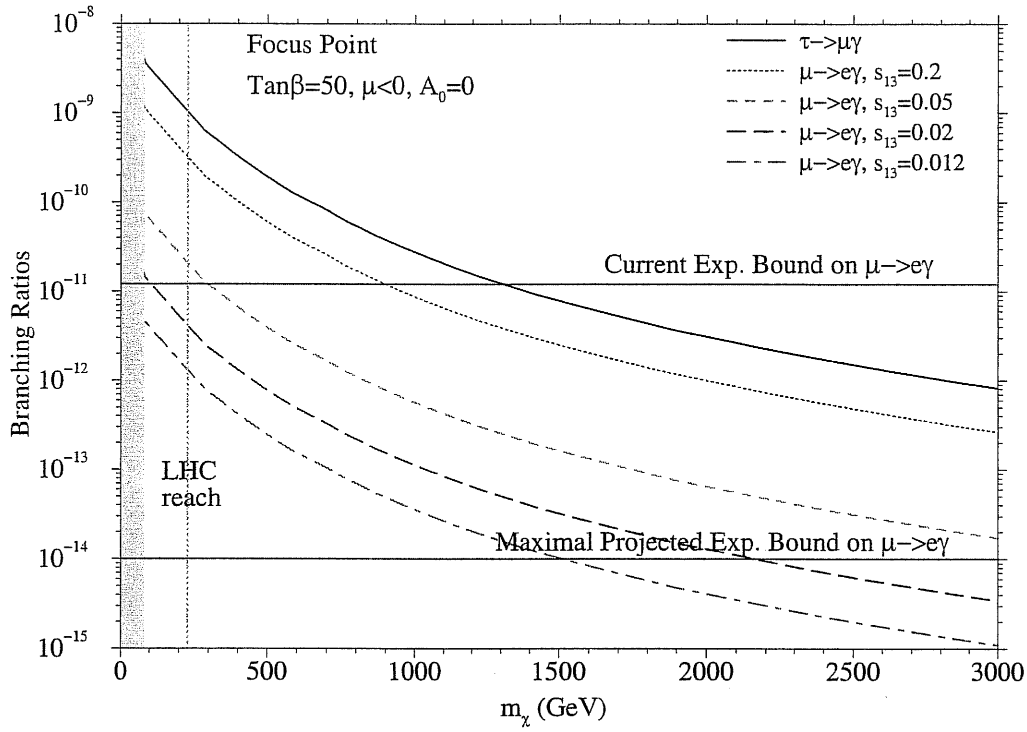

Figure 3.7: $BR(\tau \to \mu\gamma)$ and $BR(\mu \to e\gamma)$ as a function of the neutralino mass along the extreme focus point region. We set $\tan\beta = 50$, $\mu < 0$, $A_0 = 0$ and considered several values of s_{13}.

C.E.Y.

Chapter 4

Non universal gaugino masses and the fate of $\mu \to e\gamma$

4.1 Introduction

Universal gaugino masses are not a consequence of the supergravity framework but an additional assumption. Supergravity theories are determined by specifying three independent functions of the scalar fields: the superpotential, the Kahler potential, and the gauge kinetic function. In minimal supergravity models, the assumption that the vacuum expectation value of the gauge kinetic function does not break the unifying gauge symmetry leads to universal gaugino masses. Besides, mSUGRA models also postulate simple forms for the superpotential and the Kahler potential which guarantee universal boundary conditions. Such simplifying assumptions, however, are not necessarily valid; after all, in the literature there are plenty of models which do not fulfill those requirements [12]. It is then worth to consider the phenomenological implications of non minimal scenarios, and in particular of gaugino non universality.

We will limit our analysis to minimal models of gaugino non universality. A minimal model with non universal gaugino masses contains, in addition to the mSUGRA parameters $m_0, a_0, \tan\beta$, and sign μ, three gaugino masses M_1, M_2, M_3 corresponding, respectively, to the $U(1)$, $SU(2)$ and $SU(3)$ gauge groups.

So far, the discussion of these models has focused on the implications for neutralino dark matter [13] and for SUSY searches in accelerator experiments [14]. Because instead of the pure bino-like neutralino typical of mSUGRA models, the LSP may be a higgsino-like or a wino-like neutralino, models with non universal gaugino masses can handily fulfilled the cosmological bound on the relic density. In fact, wino- and higgsino-like neutralinos undergo effective annihilations into W^+W^- and Z^0Z^0, as well as coannihilations with the lightest chargino and (for the higgsino) with the next-to-lightest neutralino that easily suppress the relic abundance below the WMAP bound. Additionally, such neutralinos, due to their large couplings to the W and Z bosons, yield large direct and indirect detection rates, and therefore constitute appealing candidates for WIMP search experiments. Lepton flavor violating decays, on the other hand, have never been studied in this context.

We will investigate the implications of non universal gaugino masses on the decay $\mu \to e\gamma$. With obvious substitutions, however, our results hold also for the analogous decays $\tau \to \mu\gamma$ and $\tau \to e\gamma$. Our aim is to show that lepton flavor violating processes are sensitive to the gaugino spectrum in a non-trivial way.

To maintain our discussion as general as possible, we will not restrict ourselves to any specific model of lepton flavor violation. Instead, we will use a low energy parameterization. At low energies, the only possible sources of lepton flavor violation in the MSSM soft breaking Lagrangian are non-vanishing off-diagonal elements in $m_{\tilde{L}}^2$, $m_{\tilde{e}}^2$ and A_e. Motivated by the SUSY seesaw, we will take $m_{\tilde{e}}^2$ and A_e to be diagonal and assume that the source of lepton flavor violation resides only in the left-handed slepton mass matrix $m_{\tilde{L}}^2$. The $(2,3)$ and $(1,3)$ elements of this matrix play a subdominant role in $\mu \to e\gamma$, for they only contribute through double mass insertions and will be disregarded. The $(2,1)$ element, the relevant one, will be written in terms of the diagonal entry as

$$(m_{\tilde{L}}^2)_{21} = \delta_{\rm OD}(m_{\tilde{L}}^2)_{11} = \delta_{\rm OD}(m_{\tilde{L}}^2)_{22}, \tag{4.1}$$

being $\delta_{\rm OD}$ a free parameter. Using this parameterization, we will first study the dependence of $BR(\mu \to e\gamma)$ on the dimensionless ratios $r_2 = M_2/M_1$ and $r_3 = M_3/M_1$, defined at the GUT scale. Then, we will compute $BR(\mu \to e\gamma)$ in specific models which constrain soft terms and predict precise relations between gaugino masses. We will show that, as a result of gaugino non universality, strong cancellations often take place in $BR(\mu \to e\gamma)$.

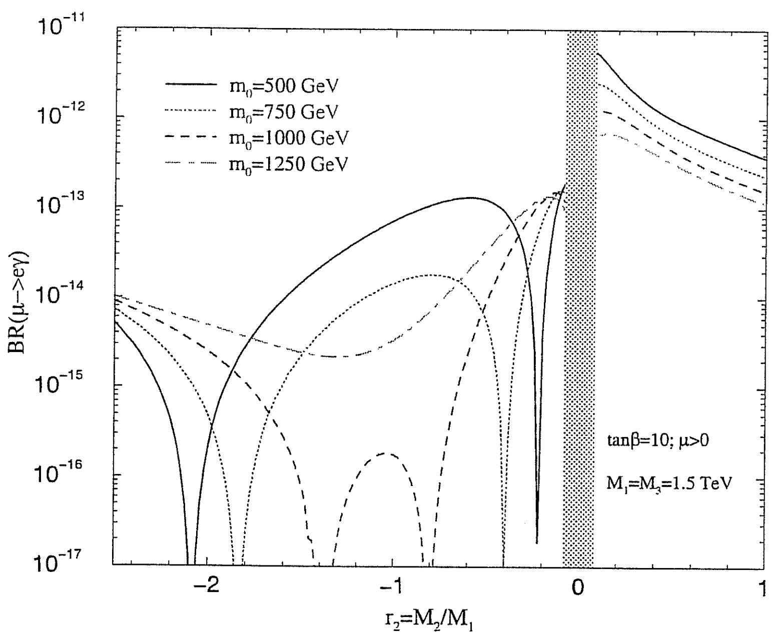

Figure 4.1: $BR(\mu \to e\gamma)$ as a function of $r_2 = M_2/M_1$ for $M_1 = M_3 = 1.5$ TeV at $\tan\beta = 10$ and $\mu > 0$ for $m_0 = 500, 750, 1000, 1250$ GeV.

4.2 Non universal wino mass term

We will begin our analysis by considering a non-universal wino mass term. That is, $M_1 = M_3$ and $M_2 = r_2 M_1$, with r_2 a free parameter. The effect of non-universality in the high energy value of the wino mass term mainly translates, at the low energy scale, into a proportional variation of M_2, and thus on the chargino and neutralino mass spectra.

As seen in fig 4.1, BR($\mu \to e\gamma$) strongly depends on r_2. In this plot we have chosen $M_1 = M_3 = 1.5$ TeV, $\tan\beta = 10$, $\mu > 0$, and different values of m_0. For $r_2 > 0$, the only effect is the suppression of BR($\mu \to$

C.E.Y.

$e\gamma$) due to heavier charginos and neutralinos. On the contrary, for $r_2 < 0$, strong cancellations occur and may suppress BR($\mu \to e\gamma$) by several orders of magnitude with respect to the mSUGRA prediction ($r_2 = 1$). As signaled by the sharp dips observed in the figure, in that region neutralino and chargino contributions have opposite signs and tend to cancel out.

The position of the dips varies with m_0 (fig 4.1) and also with $\tan\beta$ (fig 4.2) but is only slightly affected by the value of δ_{OD} (fig 4.3). This is an important result because it tells us that whether these cancellations take place or not and where they do so depend on SUSY parameters (m_0, $\tan\beta$, M_i) but not on the particular model that generates lepton flavor violating effects (δ_{OD}).

4.3 Non universal gluino mass term

Even though gluinos do not take part in the $\mu \to e\gamma$ loop, the gluino mass term does affect BR($\mu \to e\gamma$). It does so indirectly, through the electroweak symmetry breaking condition. At $\tan\beta = 10$, this condition gives

$$\mu^2 + \frac{1}{2}m_Z^2 \approx -0.1m_0^2 + 2.1M_3^2 - 0.22M_2^2 + 0.19M_2M_3 + 0.03M_1M_3 \quad (4.2)$$

and the coefficients vary rather mildly over the moderate $\tan\beta$ region. Inasmuch as the dominant contribution to the right-hand side comes from M_3, μ is practically *determined* by the gluino mass. Thus, through eq. (4.2), the gluino mass term influence chargino and neutralino masses.

In fig 4.4 we show $BR(\mu \to e\gamma)$ as a function of r_3 for different values

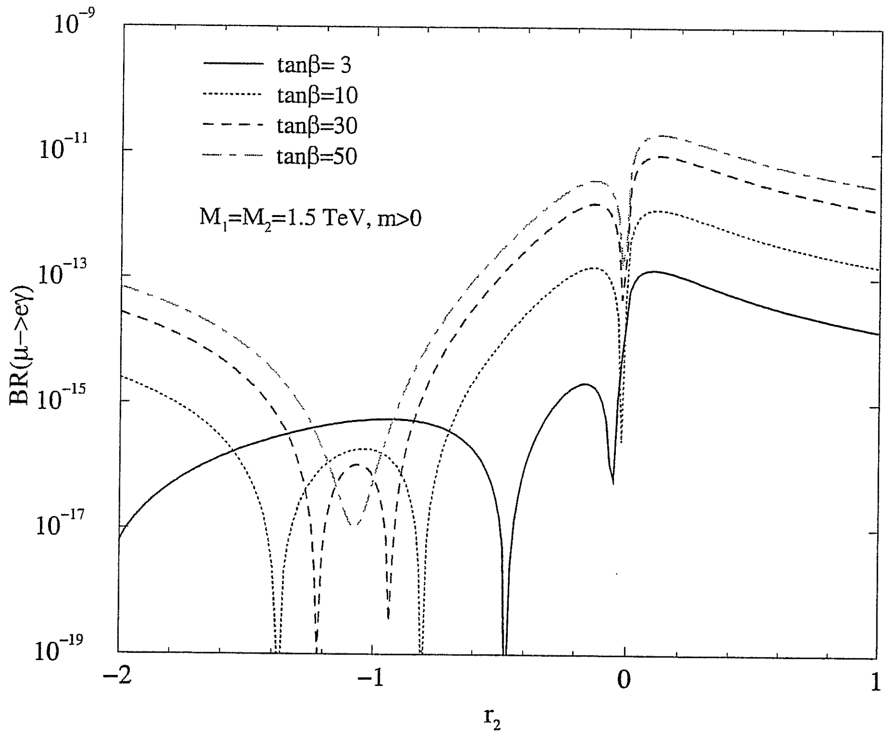

Figure 4.2: $BR(\mu \to e\gamma)$ as a function of r_2 at $M_1 = M_3 = 1.5$ TeV, $\mu > 0$ and $m_0 = 1$ TeV for different values of $\tan\beta$.

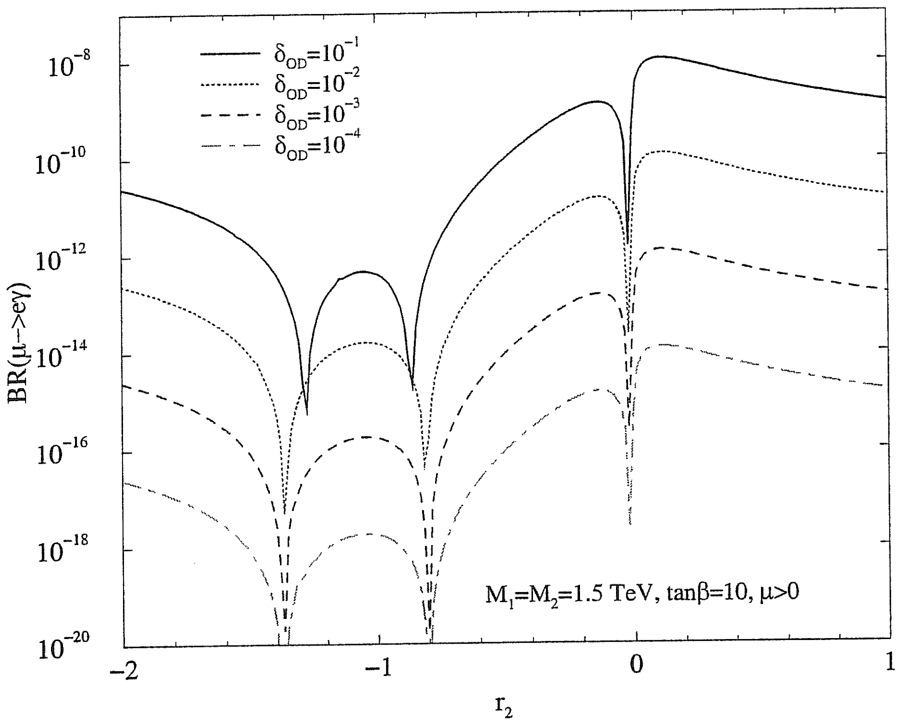

Figure 4.3: $BR(\mu \to e\gamma)$ as a function of r_2 at $M_1 = M_3 = 1.5$ TeV, $\mu > 0$, $\tan\beta = 10$, $m_0 = 1$ TeV for various δ_{OD}.

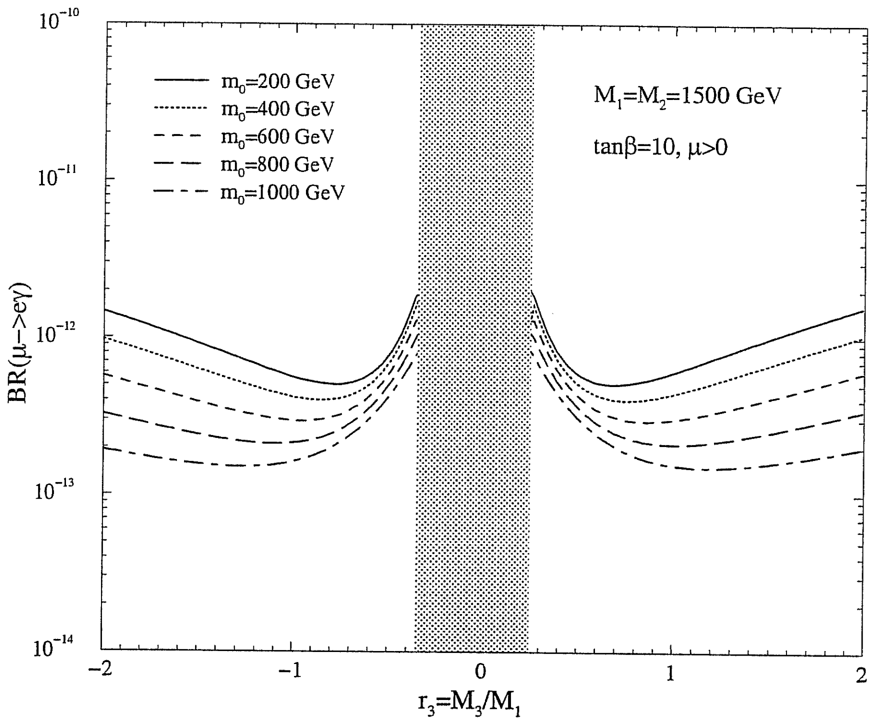

Figure 4.4: $BR(\mu \to e\gamma)$ as a function of r_3 at $M_1 = M_2 = 1.5$ TeV, $\mu > 0$ and $\tan\beta = 10$ for different values of m_0.

of m_0. Since, in agreement with eq.(4.2), the branching ratio is symmetric with respect to $r_3 \leftrightarrow -r_3$, we can limit our analysis to $r_3 > 0$. Surprisingly, the behavior of the branching is not monotonous. For small r_3, $BR(\mu \to e\gamma)$ decreases until it reaches a critical point r_c where it begins to increase. And larger values of m_0 imply larger values of r_c. To understand this peculiar behavior, we separately show in fig 4.5, the chargino and the neutralino contributions. The former decreases with r_3 whereas the latter increases. At small r_3 the branching ratio is dominated by the chargino contribution so it is decreasing, whereas at larger values the neutralino contribution dominates and the branching increases. r_c is the point where these two contributions become equal. At large r_3, therefore, the naive suppression in $BR(\mu \to e\gamma)$ due to a heavier spectrum does not take place; instead, the branching, driven by the neutralino amplitude, becomes an increasing function of r_3.

4.4 Specific Models

Until now, we have investigated $\mu \to e\gamma$ in generic models with non-universal gaugino masses. In this section, we consider two well motivated models which constrain soft breaking parameters and predict explicit relations between the three gaugino masses: $SU(5)$ GUT inspired gaugino non universality and minimal gaugino mediation.

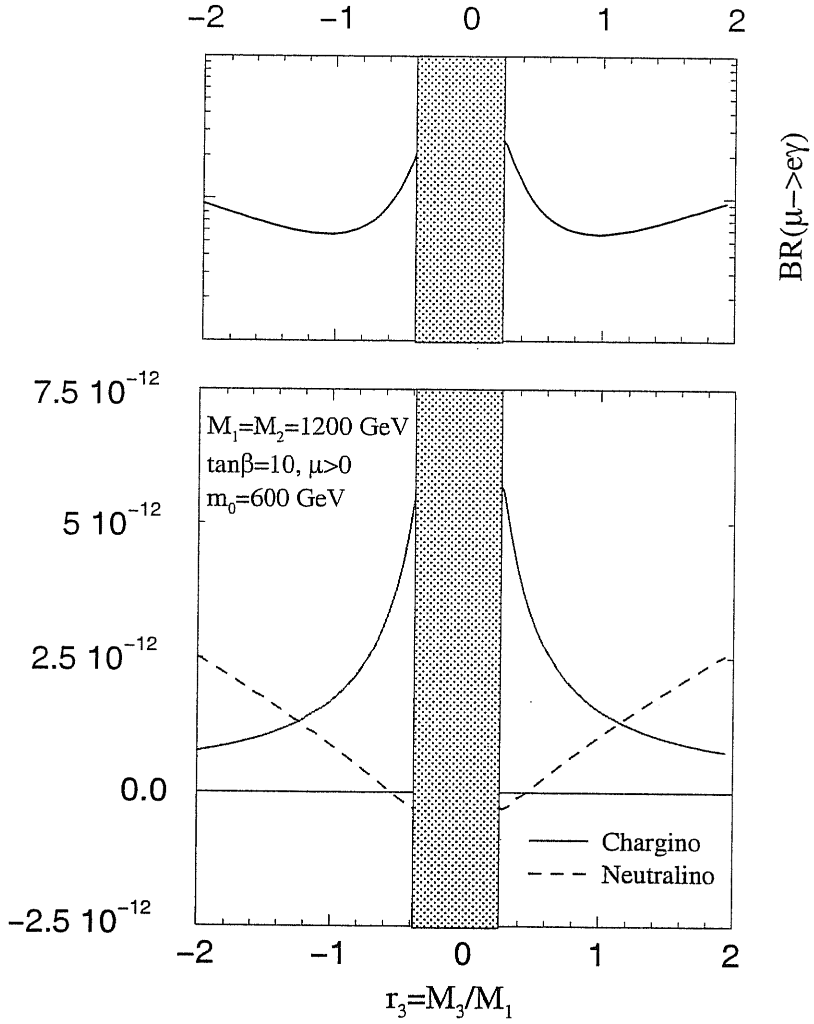

Figure 4.5: Chargino and neutralino contributions to $BR(\mu \to e\gamma)$ as a function of r_3 for $M_1 = M_2 = 1.2$ TeV, $m_0 = 600$ GeV, $\tan\beta = 10$ and $\mu > 0$.

4.4.1 SU(5)

In supergravity models, the gauge kinetic function depends on a chiral superfield ϕ, whose auxiliary F-component acquires a large vacuum expectation value. Gaugino masses come from the following five dimensional operator

$$\mathscr{L} = \frac{\langle F_\phi \rangle}{M_{\rm PL}} \lambda_i \lambda_j, \tag{4.3}$$

where $\lambda_{1,2,3}$ are the bino $\widetilde{B}$, the wino $\widetilde{W}$ and the gluino $\widetilde{g}$ fields respectively. In models based on $SU(5)$, gauginos belong to the adjoint representation of $SU(5)$, and F_ϕ can belong to any irreducible representation appearing in their symmetric product,

$$(24 \times 24)_{\rm sym} = 1 + 24 + 75 + 200\,. \tag{4.4}$$

mSUGRA models assume ϕ to be a singlet, which implies equal gaugino masses at the GUT scale. But, if ϕ belongs to one of the non-singlet representations of $SU(5)$, gaugino masses are not universal but are related to one another via representation invariants. The resulting ratios for the gaugino masses at the GUT scale are shown in Table 4.1 [15] .

The behavior of $BR(\mu \to e\gamma)$ as a function of M_3 for the different representations of $SU(5)$ is shown in fig 4.6. We do not find any cancellations. For the representations 24 and 200 the chargino and neutralino contributions have the same sign, so that they always interfere constructively. In the representation 75, where $r_2 = M_2/M_1$ is negative, the chargino amplitude dominates over the whole parameter space. Models with $SU(5)$ inspired gaugino non universality are, therefore, free of cancellations in $BR(\mu \to e\gamma)$.

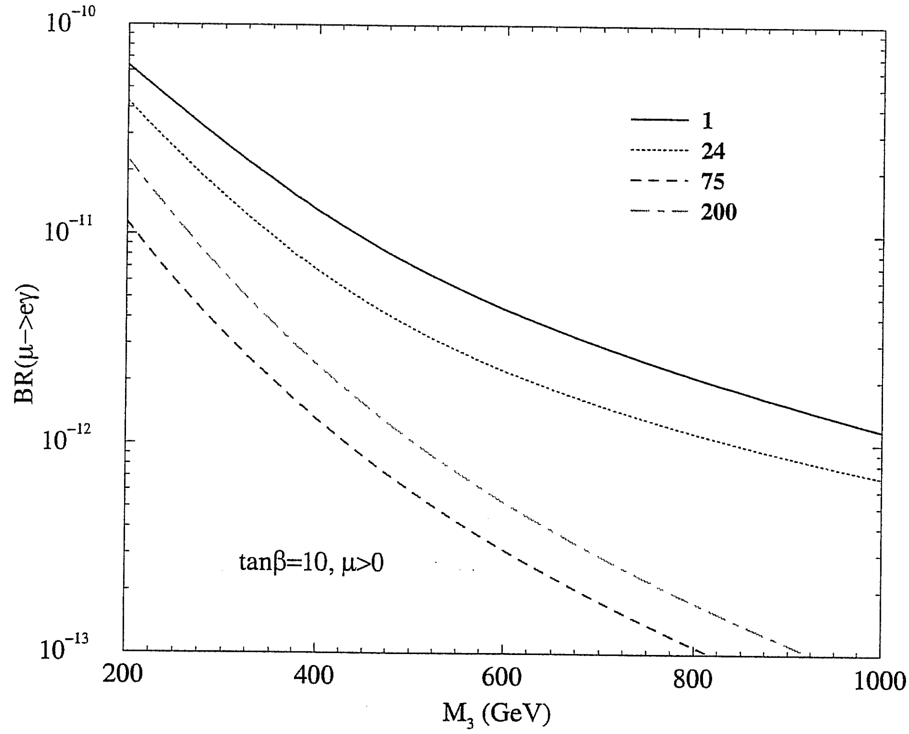

Figure 4.6: $BR(\mu \to e\gamma)$ as a function of M_3 for the different representations in the symmetric product of two $SU(5)$ adjoints. We set $m_0 = 1.2$ TeV, $\mu > 0$ and $\tan\beta = 10$.

C.E.Y.

rep	M_1	M_2	M_3
1	1	1	1
24	-1/2	-3/2	1
75	-5	3	1
200	10	2	1

Table 4.1: Relative values of the gaugino masses at the GUT scale for the different representations allowed in $SU(5)$

4.4.2 Gaugino Mediation

Models with gaugino mediated supersymmetry breaking naturally arise in higher dimensional GUT theories [16, 17, 18]. In such theories, the MSSM matter fields are localized on a *visible* brane, whereas the gauge fields propagate in the bulk of the extra dimensions. Supersymmetry, on the other hand, is broken on a distant *hidden* brane, separated from the visible one in the extra dimensions. Extradimensional locality forbids direct couplings between the two branes, and therefore suppresses all soft masses which involve MSSM matter fields – squark and slepton masses as well as trilinear couplings. Gauginos, on the contrary, can directly couple to the source of SUSY breaking, acquiring nonzero masses. Consequently, below the compactification scale, $M_c \sim 1/R$, the effective 4-dimensional theory is the MSSM, and gaugino masses are the only non-negligible sources of SUSY breaking.

If, in particular, SUSY is broken on a brane with restricted gauge symmetry, specific patterns of gaugino masses emerge. For an $SO(10)$ bulk symmetry, hidden branes with Pati-Salam $SU(4) \times SU(2)_L \times SU(2)_R$, Georgi-Glashow $SU(5) \times U(1)$, or flipped $SU(5)' \times U(1)'$ gauge symmetries can be obtained. And these symmetries link the gaugino masses of the MSSM at the compactification scale. In flipped $SU(5)$, for instance, one obtains the relation $M_3 = M_2$.

From the phenomenological point of view, models with gaugino mediation are also attractive. The flavor and CP problems of supersymmetric theories are alleviated and in a context of grand unification, the doublet-triplet splitting of Higgs fields is easily achieved and proton decay through dimension five operators is naturally suppressed.

In models with gaugino mediation, at the scale M_c, which we assume to be the unification scale ($M_c = M_{\rm GUT}$), the only free parameters are $\tan\beta$ and the gaugino masses M_i. And to avoid a charged LSP – the lightest stau – gaugino masses must necessarily be non-universal.

In fig 4.7 we show $BR(\mu \to e\gamma)$ as a function of M_2 for fixed M_1 and different values of M_3. Once again, cancellations occur when M_2 and M_1 have opposite signs. For the flipped $SU(5)$ model mentioned above, we show in fig 4.8 the branching as a function of $M_2 = M_3$ for several values of M_1. In this particular example, for any value of M_1 there exists a value of $M_2 = M_3$ for which the cancellation between chargino and neutralino contributions, and the resulting suppression of $BR(\mu \to e\gamma)$, occurs. As emerging from the figure, such value turns out to be an increasing function of M_1.

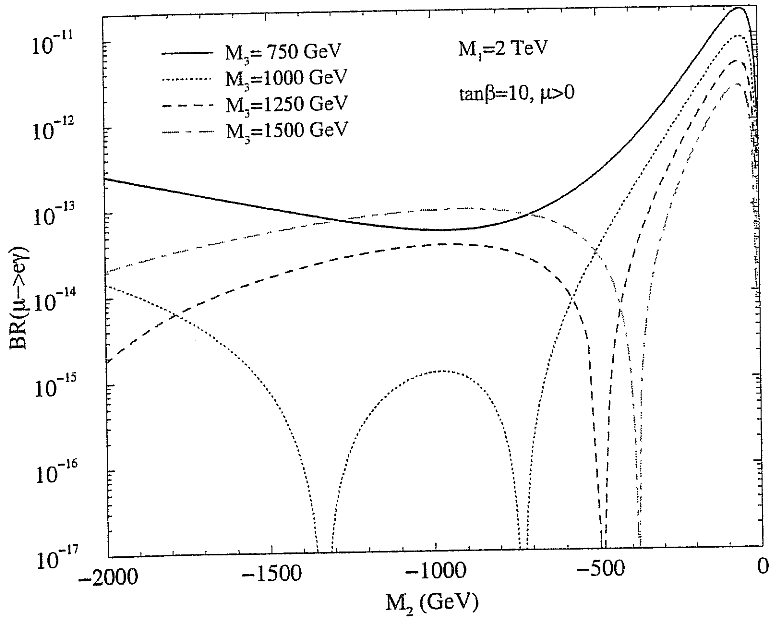

Figure 4.7: $BR(\mu \to e\gamma)$ in a model with gaugino mediation and non-universal gaugino masses at the GUT scale. We set $M_1 = 2$ TeV, $\tan\beta = 10$, $\mu > 0$ and plot the result as a function of M_2 for different values of M_3.

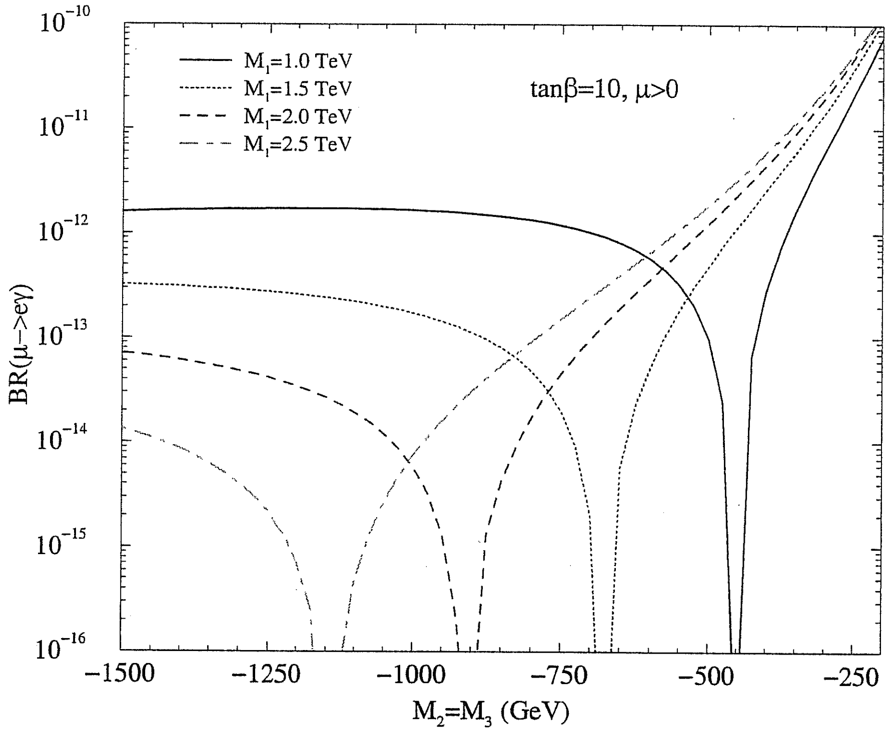

Figure 4.8: $BR(\mu \to e\gamma)$ in models with gaugino mediation and restricted flipped $SU(5)$ gauge symmetry which enforces non-universal gaugino masses and dictates $M_2 = M_3$.

C.E.Y.

4.5 Conclusion

In the context of minimal models with non universal gaugino masses, we studied the dependence of $BR(\mu \to e\gamma)$ on the gaugino spectrum. Our main finding is that when M_2 and M_1 have opposite signs, cancellations between the neutralino and the chargino contributions may suppress $BR(\mu \to e\gamma)$ by several orders of magnitude with respect to the mSUGRA prediction.

We argued that these cancellations are independent of the primary source of lepton flavor violation, and with several examples we showed that they do not require fine-tuning of supersymmetric parameters. Thus, they can be regarded as generic features of models with non universal gaugino masses.

These results may be of particular relevance for neutrino mass models. Some of them, in fact, have been ruled out because they predict, within the mSUGRA framework, too large $BR(\mu \to e\gamma)$. Non universal gaugino masses with the cancellations it brings could provide a way out to such models.

Appendix A

Renormalization Group Equations

Here we present the complete set of renormalization group equations of the MSSM with right handed neutrinos. These equations are used throughout this thesis to compute the supersymmetric spectrum and the off diagonal elements in the slepton mass matrix.

Gauge couplings:

$$16\pi^2 \frac{d}{dt}\, g_1 = \frac{33}{5}\, g_1^3 + \frac{g_1^3}{16\pi^2}\left(\frac{199}{25} g_1^2 + \frac{27}{5} g_2^2 + \frac{88}{5} g_3^2\right) , \tag{A.1}$$

$$16\pi^2 \frac{d}{dt}\, g_2 = g_2^3 + \frac{g_2^3}{16\pi^2}\left(\frac{9}{5} g_1^2 + 25 g_2^2 + 24 g_3^2\right) , \tag{A.2}$$

$$16\pi^2 \frac{d}{dt}\, g_3 = -3\, g_3^3 + \frac{g_3^3}{16\pi^2}\left(\frac{1}{5} g_1^2 + 9 g_2^2 + 14 g_3^2\right) \tag{A.3}$$

Yukawa couplings:

$$16\pi^2 \frac{d}{dt} Y_{u_{ij}} = \left\{ -\frac{13}{15} g_1^2 - 3g_2^2 - \frac{16}{3} g_3^2 + 3\,\mathrm{Tr}(Y_u Y_u^\dagger) + \mathrm{Tr}(Y_\nu Y_\nu^\dagger) \right\} Y_{u_{ij}} + 3\,(Y_u Y_u^\dagger Y_u)_{ij} + (Y_u Y_d^\dagger Y_d)_{ij} \ , \qquad \text{(A.4)}$$

$$16\pi^2 \frac{d}{dt} Y_{d_{ij}} = \left\{ -\frac{7}{15} g_1^2 - 3g_2^2 - \frac{16}{3} g_3^2 + 3\,\mathrm{Tr}(Y_d Y_d^\dagger) + \mathrm{Tr}(Y_e Y_e^\dagger) \right\} Y_{d_{ij}} + 3\,(Y_d Y_d^\dagger Y_d)_{ij} + (Y_d Y_u^\dagger Y_u)_{ij} \ , \qquad \text{(A.5)}$$

$$16\pi^2 \frac{d}{dt} Y_{e_{ij}} = \left\{ -\frac{9}{5} g_1^2 - 3g_2^2 + 3\,\mathrm{Tr}(Y_d Y_d^\dagger) + \mathrm{Tr}(Y_e Y_e^\dagger) \right\} Y_{e_{ij}} + 3\,\left(Y_e Y_e^\dagger Y_e\right)_{ij} + \left(Y_e Y_\nu^\dagger Y_\nu\right)_{ij} \ , \qquad \text{(A.6)}$$

$$16\pi^2 \frac{d}{dt} Y_{\nu_{ij}} = \left\{ -\frac{3}{5} g_1^2 - 3g_2^2 + 3\,\mathrm{Tr}\left(Y_u Y_u^\dagger\right) + \mathrm{Tr}\left(Y_\nu Y_\nu^\dagger\right) \right\} Y_{\nu_{ij}} + 3\,\left(Y_\nu Y_\nu^\dagger Y_\nu\right)_{ij} + \left(Y_\nu Y_e^\dagger Y_e\right)_{ij} \ , \qquad \text{(A.7)}$$

Gaugino masses:

$$16\pi^2 \frac{d}{dt} M_1 = \frac{66}{5}\, g_1^2 M_1 + \frac{2g_1^2}{16\pi^2} \left\{ \frac{199}{5} g_1^2\,(2M_1) + \frac{27}{5} g_2^2\,(M_1 + M_2) + \frac{88}{5} g_3^2\,(M_1 + M_3) \right\} \ , \qquad \text{(A.8)}$$

$$16\pi^2 \frac{d}{dt} M_2 = 2\, g_2^2 M_2 + \frac{2g_2^2}{16\pi^2} \left\{ \frac{9}{5} g_1^2\,(M_1 + M_2) + 25 g_2^2\,(2M_2) + 24 g_3^2\,(M_2 + M_3) \right\} \ , \qquad \text{(A.9)}$$

$$16\pi^2 \frac{d}{dt} M_3 = -6\, g_3^2 M_3 + \frac{2g_3^2}{16\pi^2} \left\{ \frac{11}{5} g_1^2\,(M_1 + M_3) + 9 g_2^2\,(M_2 + M_3) + 14 g_3^2\,(2M_3) \right\} \ , \qquad \text{(A.10)}$$

C.E.Y.

Sfermion masses:

$$16\pi^2\frac{d}{dt}\left(m^2_{\tilde{Q}}\right)_{ij} = -\left(\frac{2}{15}g_1^2\left|M_1\right|^2+6g_2^2\left|M_2\right|^2+\frac{32}{3}g_3^2\left|M_3\right|^2\right)\delta_{ij}+\frac{1}{5}g_1^2\ S\ \delta_{ij}$$
$$+\left(m^2_{\tilde{Q}}Y_u^\dagger Y_u+m^2_{\tilde{Q}}Y_d^\dagger Y_d+Y_u^\dagger Y_u m^2_{\tilde{Q}}+Y_d^\dagger Y_d m^2_{\tilde{Q}}\right)_{ij}$$
$$+2\left(Y_u^\dagger m^2_{\tilde{u}}Y_u+m^2_{H_u}Y_u^\dagger Y_u+A_u^\dagger A_u\right)_{ij}$$
$$+2\left(Y_d^\dagger m^2_{\tilde{d}}Y_d+m^2_{H_d}Y_d^\dagger Y_d+A_d^\dagger A_d\right)_{ij}\ , \tag{A.11}$$

$$16\pi^2\frac{d}{dt}\left(m^2_{\tilde{u}}\right)_{ij} = -\left(\frac{32}{15}g_1^2\left|M_1\right|^2+\frac{32}{3}g_3^2\left|M_3\right|^2\right)\delta_{ij}-\frac{4}{5}g_1^2\ S\ \delta_{ij}$$
$$+2\left(m^2_{\tilde{u}}Y_uY_u^\dagger+Y_uY_u^\dagger m^2_{\tilde{u}}\right)_{ij}$$
$$+4\left(Y_u m^2_{\tilde{Q}}Y_u^\dagger+m^2_{H_u}Y_uY_u^\dagger+A_uA_u^\dagger\right)_{ij}\ , \tag{A.12}$$

$$16\pi^2\frac{d}{dt}\left(m^2_{\tilde{d}}\right)_{ij} = -\left(\frac{8}{15}g_1^2\left|M_1\right|^2+\frac{32}{3}g_3^2\left|M_3\right|^2\right)\delta_{ij}+\frac{2}{5}g_1^2\ S\ \delta_{ij}$$
$$+2\left(m^2_{\tilde{d}}Y_dY_d^\dagger+Y_dY_d^\dagger m^2_{\tilde{d}}\right)_{ij}$$
$$+4\left(Y_d m^2_{\tilde{Q}}Y_d^\dagger+m^2_{H_d}Y_dY_d^\dagger+A_dA_d^\dagger\right)_{ij}\ , \tag{A.13}$$

$$16\pi^2\frac{d}{dt}\left(m^2_{\tilde{L}}\right)_{ij} = -\left(\frac{6}{5}g_1^2\left|M_1\right|^2+6g_2^2\left|M_2\right|^2\right)\delta_{ij}-\frac{3}{5}g_1^2\ S\ \delta_{ij}$$
$$+\left(m^2_{\tilde{L}}Y_e^\dagger Y_e+m^2_{\tilde{L}}Y_\nu^\dagger Y_\nu+Y_e^\dagger Y_e m^2_{\tilde{L}}+Y_\nu^\dagger Y_\nu m^2_{\tilde{L}}\right)_{ij}$$
$$+2\left(Y_e^\dagger m^2_{\tilde{e}}Y_e+m^2_{H_d}Y_e^\dagger Y_e+A_e^\dagger A_e\right)_{ij}$$
$$+2\left(Y_\nu^\dagger m^2_{\tilde{\nu}}Y_\nu+m^2_{H_u}Y_\nu^\dagger Y_\nu+A_\nu^\dagger A_\nu\right)_{ij}\ , \tag{A.14}$$

$$16\pi^2\frac{d}{dt}\left(m^2_{\tilde{e}}\right)_{ij} = -\frac{24}{5}g_1^2\left|M_1\right|^2\delta_{ij}+\frac{6}{5}g_1^2\ S\ \delta_{ij}+2\left(m^2_{\tilde{e}}Y_eY_e^\dagger+Y_eY_e^\dagger m^2_{\tilde{e}}\right)_{ij}$$
$$+4\left(Y_e m^2_{\tilde{L}}Y_e^\dagger+m^2_{H_d}Y_eY_e^\dagger+A_eA_e^\dagger\right)_{ij}\ , \tag{A.15}$$

$$16\pi^2\frac{d}{dt}\left(m^2_{\tilde{\nu}}\right)_{ij} = 2\left(m^2_{\tilde{\nu}}Y_\nu Y_\nu^\dagger+Y_\nu Y_\nu^\dagger m^2_{\tilde{\nu}}\right)_{ij}+4\left(Y_\nu m^2_{\tilde{L}}Y_\nu^\dagger+m^2_{H_u}Y_\nu Y_\nu^\dagger+A_\nu A_\nu^\dagger\right)_{ij}\ , \tag{A.16}$$

C.E.Y.

Trilinear couplings:

$$16\pi^2\frac{d}{dt}A_{e_{ij}} = \left\{-\frac{9}{5}g_1^2 - 3g_2^2 + 3\mathrm{Tr}(Y_d^\dagger Y_d) + \mathrm{Tr}(Y_e^\dagger Y_e)\right\} A_{e_{ij}}$$
$$+2\left\{\frac{9}{5}g_1^2 M_1 + 3g_2^2 M_2 + 3\mathrm{Tr}(Y_d^\dagger A_d) + \mathrm{Tr}(Y_e^\dagger A_e)\right\} Y_{e_{ij}}$$
$$+4\left(Y_e Y_e^\dagger A_e\right)_{ij} + 5\left(A_e Y_e^\dagger Y_e\right)_{ij} + 2\left(Y_e Y_\nu^\dagger A_\nu\right)_{ij} + \left(A_e Y_\nu^\dagger Y_\nu\right)_{ij} \quad \text{(A.17)}$$

$$16\pi^2\frac{d}{dt}A_{\nu_{ij}} = \left\{-\frac{3}{5}g_1^2 - 3g_2^2 + 3\mathrm{Tr}(Y_u^\dagger Y_u) + \mathrm{Tr}(Y_\nu^\dagger Y_\nu)\right\} A_{\nu_{ij}}$$
$$+2\left\{\frac{3}{5}g_1^2 M_1 + 3g_2^2 M_2 + 3\mathrm{Tr}(Y_u^\dagger A_u) + \mathrm{Tr}(Y_\nu^\dagger A_\nu)\right\} Y_{\nu_{ij}}$$
$$+4(Y_\nu Y_\nu^\dagger A_\nu)_{ij} + 5(A_\nu Y_\nu^\dagger Y_\nu)_{ij} + 2(Y_\nu Y_e^\dagger A_e)_{ij} + (A_\nu Y_e^\dagger Y_e)_{ij} \quad \text{(A.18)}$$

$$16\pi^2\frac{d}{dt}A_{u_{ij}} = \left\{-\frac{13}{15}g_1^2 - 3g_2^2 - \frac{16}{3}g_3^2 + 3\mathrm{Tr}(Y_u^\dagger Y_u) + \mathrm{Tr}(Y_\nu^\dagger Y_\nu)\right\} A_{u_{ij}}$$
$$+2\left\{\frac{13}{15}g_1^2 M_1 + 3g_2^2 M_2 + \frac{16}{3}g_3^2 M_3 + 3\mathrm{Tr}(Y_u^\dagger A_u) + \mathrm{Tr}(Y_\nu^\dagger A_\nu)\right\} Y_{u_{ij}}$$
$$+4(Y_u Y_u^\dagger A_u)_{ij} + 5(A_u Y_u^\dagger Y_u)_{ij} + 2(Y_u Y_d^\dagger A_d)_{ij} + (A_u Y_d^\dagger Y_d)_{ij} \quad \text{(A.19)}$$

$$16\pi^2\frac{d}{dt}A_{d_{ij}} = \left\{-\frac{7}{15}g_1^2 - 3g_2^2 - \frac{16}{3}g_3^2 + 3\mathrm{Tr}(Y_d^\dagger Y_d) + \mathrm{Tr}(Y_e^\dagger Y_e)\right\} A_{d_{ij}}$$
$$+2\left\{\frac{7}{15}g_1^2 M_1 + 3g_2^2 M_2 + \frac{16}{3}g_3^2 M_3 + 3\mathrm{Tr}(Y_d^\dagger A_d) + \mathrm{Tr}(Y_e^\dagger A_e)\right\} Y_{d_{ij}}$$
$$+4(Y_d Y_d^\dagger A_d)_{ij} + 5(A_d Y_d^\dagger Y_d)_{ij} + 2(Y_d Y_u^\dagger A_u)_{ij} + (A_d Y_u^\dagger Y_u)_{ij} \quad \text{(A.20)}$$

C.E.Y.

Higgs masses:

$$16\pi^2 \frac{d}{dt}(m_{H_u}^2) = -\left(\frac{6}{5}g_1^2 |M_1|^2 + 6g_2^2 |M_2|^2\right) + \frac{3}{5}g_1^2 S$$
$$+6\,\mathrm{Tr}\left(m_{\tilde{Q}}^2 Y_u^\dagger Y_u + Y_u^\dagger (m_{\tilde{u}}^2 + m_{H_u}^2) Y_u + A_u^\dagger A_u\right)$$
$$+2\,\mathrm{Tr}\left(m_{\tilde{L}}^2 Y_\nu^\dagger Y_\nu + Y_\nu^\dagger (m_{\tilde{\nu}}^2 + m_{H_u}^2) Y_\nu + A_\nu^\dagger A_\nu\right), \quad \text{(A.21)}$$

$$16\pi^2 \frac{d}{dt}(m_{H_d}^2) = -\left(\frac{6}{5}g_1^2 |M_1|^2 + 6g_2^2 |M_2|^2\right) - \frac{3}{5}g_1^2 S$$
$$+6\,\mathrm{Tr}\left(m_{\tilde{Q}}^2 Y_d^\dagger Y_d + Y_d^\dagger (m_{\tilde{d}}^2 + m_{H_d}^2) Y_d + A_d^\dagger A_d\right)$$
$$+2\,\mathrm{Tr}\left(m_{\tilde{L}}^2 Y_e^\dagger Y_e + Y_e^\dagger (m_{\tilde{e}}^2 + m_{H_d}^2) Y_e + A_e^\dagger A_e\right), \quad \text{(A.22)}$$

where

$$S = \mathrm{Tr}(m_{\tilde{Q}}^2 + m_{\tilde{d}}^2 - 2m_{\tilde{u}}^2 - m_{\tilde{L}}^2 + m_{\tilde{e}}^2) - m_{H_d}^2 + m_{H_u}^2 \ , \quad \text{(A.23)}$$

and we have used the GUT convention for the $U(1)$ gauge coupling constant, g_1, and $t = \ln\mu$ where μ is denoted as the renormalization point.

Appendix B

Notations in the MSSM

In this appendix, we present our conventions for the MSSM.

The chargino mass matrix has the following form:

$$-\mathscr{L}_m = \left(\overline{\widetilde{W}_R^-}\ \overline{\widetilde{H}_{2R}^-}\right) M_C \begin{pmatrix} \widetilde{W}_L^- \\ \widetilde{H}_{1L}^- \end{pmatrix} + h.c. \ , \tag{B.1}$$

where

$$M_C = \begin{pmatrix} M_2 & \sqrt{2} m_W \cos\beta \\ \sqrt{2} m_W \sin\beta & \mu \end{pmatrix} \ . \tag{B.2}$$

This matrix can be diagonalized by two 2×2 real orthogonal matrices O_L and O_R according to:

$$O_R M_C O_L^{\mathsf{T}} = \text{diagonal} \ . \tag{B.3}$$

If we define

$$\begin{pmatrix} \widetilde{\chi}_{1L}^- \\ \widetilde{\chi}_{2L}^- \end{pmatrix} = O_L \begin{pmatrix} \widetilde{W}_L^- \\ \widetilde{H}_{1L}^- \end{pmatrix} \ , \qquad \begin{pmatrix} \widetilde{\chi}_{1R}^- \\ \widetilde{\chi}_{2R}^- \end{pmatrix} = O_R \begin{pmatrix} \widetilde{W}_R^- \\ \widetilde{H}_{2R}^- \end{pmatrix} \ , \tag{B.4}$$

then

$$\widetilde{\chi}_A^- = \widetilde{\chi}_{AL}^- + \widetilde{\chi}_{AR}^- \tag{B.5}$$

forms a Dirac fermion with mass $M_{\widetilde{\chi}_A^-}$.

The mass matrix of the neutralino sector is given by

$$-\mathscr{L}_m = \frac{1}{2}\left(\widetilde{B}_L \widetilde{W}_L^0 \widetilde{H}_{1L}^0 \widetilde{H}_{2L}^0\right) M_N \begin{pmatrix} \widetilde{B}_L \\ \widetilde{W}_L^0 \\ \widetilde{H}_{1L}^0 \\ \widetilde{H}_{2L}^0 \end{pmatrix} + h.c. \ , \tag{B.6}$$

where

$$M_N = \begin{pmatrix} M_1 & 0 & -m_Z \sin\theta_W \cos\beta & m_Z \sin\theta_W \sin\beta \\ 0 & M_2 & m_Z \cos\theta_W \cos\beta & -m_Z \cos\theta_W \sin\beta \\ -m_Z \sin\theta_W \cos\beta & m_Z \cos\theta_W \cos\beta & 0 & -\mu \\ m_Z \sin\theta_W \sin\beta & -m_Z \cos\theta_W \sin\beta & -\mu & 0 \end{pmatrix} . \tag{B.7}$$

We can diagonalize M_N with a real orthogonal matrix O_N:

$$O_N M_N O_N^{\mathsf{T}} = \text{diagonal} \ . \tag{B.8}$$

The mass eigenstates are given by

$$\widetilde{\chi}_{BL}^0 = (O_N)_{BC} \widetilde{X}_{CL}^0 \ \ (B, C = 1, \cdots, 4) \ \ ; \ \widetilde{X}_{CL}^0 = (\widetilde{B}_L, \widetilde{W}_L^0, \widetilde{H}_{1L}^0, \widetilde{H}_{2L}^0) \ . \tag{B.9}$$

We have four Majorana spinors

$$\widetilde{\chi}_B^0 = \widetilde{\chi}_{BL}^0 + \widetilde{\chi}_{BR}^0 \ , \qquad (B = 1, \cdots, 4) \tag{B.10}$$

C.E.Y.

with masses $M_{\tilde{\chi}^0_B}$.

The slepton mass matrix can be cast in the following form:

$$-\mathscr{L}_s = \left(\tilde{e}_L^\dagger, \tilde{e}_R^\dagger\right) \begin{pmatrix} m_L^2 & m_{LR}^{2\dagger} \\ m_{LR}^2 & m_R^2 \end{pmatrix} \begin{pmatrix} \tilde{e}_L \\ \tilde{e}_R \end{pmatrix} , \tag{B.11}$$

with

$$\left(m_L^2\right)_{ij} = \left(m_{\tilde{L}}^2\right)_{ij} + m_{e_i}^2 \delta_{ij} - m_Z^2 \cos 2\beta \left(\frac{1}{2} + \sin^2\theta_W\right) \delta_{ij} , \tag{B.12}$$

$$\left(m_R^2\right)_{ij} = \left(m_{\tilde{e}}^2\right)_{ij} + m_{e_i}^2 \delta_{ij} - m_Z^2 \cos 2\beta \sin^2\theta_W \delta_{ij} , \tag{B.13}$$

$$\left(m_{LR}^2\right)_{ij} = \frac{v \cos\beta}{\sqrt{2}} A_{eij} - m_{e_i} \mu \tan\beta \delta_{ij} . \tag{B.14}$$

We diagonalize the slepton mass matrix, M_L^2, by a 6×6 real orthogonal matrix U^l as

$$U^l M_L^2 U^{l\mathsf{T}} = \text{diag.}\left(m_{\tilde{l}_1}^2, \cdots, m_{\tilde{l}_6}^2\right) , \tag{B.15}$$

A mass eigenstate is then written as

$$\tilde{l}_Y = U^l_{Y,i} \tilde{l}_{Li} + U^l_{Y,i+3} \tilde{l}_{Ri} , \qquad (Y = 1, \cdots, 6) . \tag{B.16}$$

Since there are no right-handed sneutrinos at low energies, the sneutrino mass matrix is

$$(M_{\tilde{\nu}}^2)_{ij} = \left(m_{\tilde{L}}^2\right)_{ij} + \frac{1}{2} m_Z^2 \cos 2\beta \delta_{ij} . \tag{B.17}$$

The diagonalization is carried out by a 3×3 orthogonal matrix U^ν

$$U^\nu M_{\tilde{\nu}}^2 U^{\nu\mathsf{T}} = \text{diag.} \tag{B.18}$$

and the mass eigenstates read

$$\tilde{\nu}_X = U^\nu_{X,i} \tilde{\nu}_{Li}, \quad X = 1, 2, 3. \tag{B.19}$$

Appendix C

The process $\ell_j \to \ell_i\gamma$

The amplitude for the process $\ell_j \to \ell_i\gamma$ is written as

$$T = e\epsilon^{\alpha *}\bar{u}_i(p-q)\left[m_j i\sigma_{\alpha\beta}q^\beta(A^L P_L + A^R P_R)\right]u_\mu(p) \tag{C.1}$$

where q is the momentum of the photon, e is the electric charge, ϵ^* the photon polarization vector, u_i and u_j the wave functions of the initial and final leptons, and p is the momentum of the particle ℓ_j.

Each coefficient in the above formula receives contributions from the neutralino and the chargino diagrams and therefore can be written as:

$$A_{L,R} = A^{(c)}_{L,R} + A^{(n)}_{L,R}\ , \tag{C.2}$$

$$A^{(c)}_L = -\frac{1}{32\pi^2}\sum_{A,X}\frac{1}{m^2_{\tilde{\nu}_X}}\left[C^{L(l)}_{jAX}C^{L(l)*}_{iAX}k_1(x_{AX}) + C^{L(l)}_{jAX}C^{R(l)*}_{iAX}\frac{M_{\tilde{\chi}^-_A}}{m_j}k_2(x_{AX})\right] \tag{C.3}$$

$$A^{(n)}_L = \frac{1}{32\pi^2}\sum_{B,Y}\frac{1}{m^2_{\tilde{l}_Y}}\left[N^{L(l)}_{jBY}N^{L(l)*}_{iBY}k_3(y_{BY}) + N^{L(l)}_{jBY}N^{R(l)*}_{iBY}\frac{M_{\tilde{\chi}^0_B}}{m_i}k_4(y_{BY})\right] \tag{C.4}$$

$$A^{(c,n)}_R = A^{(c,n)}_L\Big|_{L\leftrightarrow R}\ . \tag{C.5}$$

where the dimensionless parameters x_{AX} and y_{BY} are defined as

$$x_{AX} = \frac{M^2_{\tilde{\chi}^-_A}}{m^2_{\tilde{\nu}_X}} \quad , \qquad y_{BY} = \frac{M^2_{\tilde{\chi}^0_B}}{m^2_{\tilde{l}_Y}} \quad , \tag{C.6}$$

the coefficients in Eqs. (C.3) and (C.4) are given by

$$C^{L(l)}_{iAX} = g_2 \frac{m_{l_i}}{\sqrt{2} m_W \cos\beta} (O_L)_{A2} U^{\nu}_{X,i} \ , \tag{C.7}$$

$$C^{R(l)}_{iAX} = -g_2 (O_R)_{A1} U^{\nu}_{X,i} \ , \tag{C.8}$$

$$N^{L(l)}_{iBY} = -\frac{g_2}{\sqrt{2}} \left\{ \frac{m_{l_i}}{m_W \cos\beta} (O_N)_{B3} U^l_{Y,i} + 2 (O_N)_{B1} \tan\theta_W U^l_{Y,i+3} \right\} \ , \tag{C.9}$$

$$N^{R(l)}_{iBY} = -\frac{g_2}{\sqrt{2}} \left\{ [-(O_N)_{B2} - (O_N)_{B1} \tan\theta_W] U^l_{Y,i} + \frac{m_{l_i}}{m_W \cos\beta} (O_N)_{B3} U^l_{Y,i+3} \right\} \tag{C.10}$$

and the functions $k_i(x)$ are defined as

$$k_1(x) = \frac{1}{6(1-x)^4} (2 + 3x - 6x^2 + x^3 + 6x \ln x) \tag{C.11}$$

$$k_2(x) = \frac{1}{(1-x)^3} (-3 + 4x - x^2 - 2 \ln x) \tag{C.12}$$

$$k_3(x) = \frac{1}{6(1-x)^4} (1 - 6x + 3x^2 + 2x^3 - 6x^2 \ln x) \tag{C.13}$$

$$k_4(x) = \frac{1}{(1-x)^3} (1 + x^2 + 2x \ln x) \tag{C.14}$$

The width of the decay $l_j \to l_i\gamma$ is easily calculated from the amplitude

$$\Gamma(l_j \to l_i\gamma) = \frac{\alpha}{4\pi} m^5_{\ell_j} \left(|A_L|^2 + |A_R|^2 \right) \ , \tag{C.15}$$

where $\alpha = e^2/4\pi$.

Finally, the function $g(x)$ used in eq (2.6) is given by

$$g(x) = k_2(x) + x k_2'(x). \tag{C.16}$$

C.E.Y.

Bibliography

[1] S. Pascoli, S. T. Petcov and C. E. Yaguna, Phys. Lett. B **564** (2003) 241 [arXiv:hep-ph/0301095].

[2] S. T. Petcov, S. Profumo, Y. Takanishi and C. E. Yaguna, Nucl. Phys. B **676** (2004) 453 [arXiv:hep-ph/0306195].

[3] S. Profumo and C. E. Yaguna, Nucl. Phys. B **681** (2004) 247 [arXiv:hep-ph/0307225].

[4] A. Masiero, S. Profumo, S. K. Vempati and C. E. Yaguna, JHEP **0403** (2004) 046 [arXiv:hep-ph/0401138].

[5] S. M. Bilenky and S. T. Petcov, Rev. Mod. Phys. **59** (1987) 671 [Erratum-ibid. **61** (1989) 169].

[6] F. Borzumati and A. Masiero, Phys. Rev. Lett. **57** (1986) 961.

[7] A. Masiero, S. K. Vempati and O. Vives, Nucl. Phys. B **649** (2003) 189 [arXiv:hep-ph/0209303].

[8] D. N. Spergel *et al.* [WMAP Collaboration], Astrophys. J. Suppl. **148** (2003) 175 [arXiv:astro-ph/0302209].

[9] H. Baer, A. Belyaev, T. Krupovnickas and A. Mustafayev, JHEP **0406** (2004) 044 [arXiv:hep-ph/0403214].

[10] M. Davier, S. Eidelman, A. Hocker and Z. Zhang, Eur. Phys. J. C **31** (2003) 503 [arXiv:hep-ph/0308213].

[11] K. Hagiwara, A. D. Martin, D. Nomura and T. Teubner, Phys. Rev. D **69** (2004) 093003 [arXiv:hep-ph/0312250].

[12] H. Baer, M. A. Diaz, P. Quintana and X. Tata, JHEP **0004** (2000) 016 [arXiv:hep-ph/0002245].

[13] V. Bertin, E. Nezri and J. Orloff, JHEP **0302** (2003) 046 [arXiv:hep-ph/0210034].

[14] N. V. Krasnikov and S. I. Bityukov, arXiv:hep-ph/0110015.

[15] G. Anderson, C. H. Chen, J. F. Gunion, J. Lykken, T. Moroi and Y. Yamada, arXiv:hep-ph/9609457.

[16] D. E. Kaplan, G. D. Kribs and M. Schmaltz, Phys. Rev. D **62** (2000) 035010 [arXiv:hep-ph/9911293].

[17] Z. Chacko, M. A. Luty, A. E. Nelson and E. Ponton, JHEP **0001** (2000) 003 [arXiv:hep-ph/9911323].

C.E.Y.

[18] M. Schmaltz and W. Skiba, Phys. Rev. D **62** (2000) 095005 [arXiv:hep-ph/0001172].

[19] S. Komine and M. Yamaguchi, Phys. Rev. D **63** (2001) 035005 [arXiv:hep-ph/0007327].

[20] H. Baer, C. Balazs, A. Belyaev, R. Dermisek, A. Mafi and A. Mustafayev, JHEP **0205** (2002) 061 [arXiv:hep-ph/0204108].